Reduced gas seepages in ophiolitic complexes: Evidences for multiple origins of the H 2 -CH 4 -N 2 gas mixtures

Christèle Vacquand, Eric Deville, Valérie Beaumont, François Guyot, Olivier Sissmann, Daniel Pillot, Carlo Arcilla, Alain Prinzhofer

Reduced gas seepages in ophiolitic complexes: Evidences for multiple origins of the H_2-CH_4-N_2 gas mixtures

Christèle Vacquand[a], Eric Deville[a], Valérie Beaumont[a], François Guyot[b], Olivier Sissmann[a], Daniel Pillot[a], Carlo Arcilla[c], Alain Prinzhofer[a, d]

[a] *IFP Energies nouvelles, 1 & 4 avenue de Bois-Préau, 92852 Rueil-Malmaison Cedex, France*

[b] *IMPMC, Sorbonne Universités, MNHN, UPMC, CNRS, 61 rue Buffon, 75005 Paris, France*

[c] *National Institute of Geological Sciences, University of the Philippines, Diliman, Quezon City, Philippines*

[d] *Present address: GEO4U, Praia de Botafogo 501, 22250-040 Rio de Janeiro, Brazil*

Key-words: ophiolite, serpentinization, hydrogen, abiotic methane, deep nitrogen

---

Corresponding author: Eric Deville
E-mail address: eric.deville@ifpen.fr
Telephone number: +33 1 47 52 69 54

Highlights

⇨ Gas generation during serpentinization
⇨ Deep origin of nitrogen seepages in obducted ophiolitic complexes
⇨ Multiple sources of gas and gas mixing in ophiolitic complexes
⇨ Multiple sources of carbon during abiotic methane generation

ABSTRACT

This paper proposes a comparative study of reduced gas seepages occurring in ultrabasic to basic rocks outcropping in ophiolitic complexes based on the study of seepages from Oman, the Philippines, Turkey and New Caledonia. This study is based on analyses of the gas chemical composition, noble gases contents, stable isotopes of carbon, hydrogen and nitrogen. These seepages are mostly made of mixtures of three main components which are H_2, CH_4 and N_2 in various proportions. The relative contents of the three main gas components show 4 distinct types of gas mixtures (H_2-rich, N_2-rich, N_2-H_2-CH_4 and H_2-CH_4). These types are interpreted as reflecting different zones of gas generation within or below the ophiolitic complexes. In the H_2-rich type associated noble gases display signatures close to the value of air. In addition to the atmospheric component, mantle and crustal contributions are present in the N_2-rich, N_2-H_2-CH_4 and H_2-CH_4 types. H_2-bearing gases are either associated with ultra-basic (pH 10-12) spring waters or they seep directly in fracture systems from the ophiolitic rocks. In ophiolitic contexts, ultrabasic rocks provide an adequate environment with available Fe^{2+} and alkaline conditions that favor H_2 production. CH_4 is produced either directly by reaction of dissolved CO_2 with basic-ultrabasic rocks during the serpentinization process or in a second step by H_2-CO_2 interaction. H_2 is present in the gas when no more carbon is available in the system to generate CH_4. The N_2-rich type is notably associated with relatively high contents of crustal ^4He and in this gas type N_2 is interpreted as issued mainly from sediments located below the ophiolitic units.

Introduction

Serpentinization generates natural emission of H_2 on Earth. The process is inherent to exposure of reduced mantle rocks to hydration conditions in a wide range of thermal conditions, at least up to the critical temperature of water (374°C). This occurs commonly at mid-oceanic ridges where hydrothermal fluid circulation at high temperature provides conditions for ferromagnesian mineral alteration. Indeed, at mid-oceanic ridges H_2-rich fluids are associated with N_2 and CH_4 contents and on black smokers with CO_2 (Welhan and Craig, 1979; Kelley and Früh-Green, 1999; Charlou et al., 2002; Kelley et al., 2001, 2005; Gallant and Von Damm, 2006; Kumagai et al., 2008; and others). Natural H_2 seepages are also reported onshore, in former oceanic rocks present in ophiolite complexes. Notably, H_2 seepages associated with these ultrabasic rocks have been reported in the Sultanate of Oman (Neal and Stanger, 1983; Sano et al., 1993; Vacquand, 2011; Boulart et al., 2013; Miller et al., 2016), the Philippines (Abrajano et al. 1988, 1990) and Turkey (De Boer et al., 2007; Hosgörmez et al., 2008; Etiope et al., 2011). These gas seepages are often associated with ultra-basic springs (pH 10-12) that are present in many basic-ultrabasic rock exposures. Such ultra-basic waters have been interpreted as evidences of active serpentinization (Barnes et al., 1967, 1978; Neal and Stanger, 1983; Abrajano et al., 1988, 1990; Sano et al., 1993; Bruni et al., 2002; Cipolli et al., 2004; Deville et al., 2011; Szponar et al., 2013; Etiope et al., 2013; Chavagnac et al., 2013; Cardace et al., 2015; Meyer-Dombard et al., 2015; Woycheese et al., 2015; Deville and Prinzhofer, 2016). In these cases, H_2-rich gas is either dissolved or present as free gas bubbling in the ultra-basic water. In other cases, H_2-rich gas seepages occur in rock fractures and can locally burn spontaneously. This is notably the case of the famous Chimaera near Antalya, place of the first Olympic flame, which are known to be burning since antiquity (De Boer et al., 2007; Hosgörmez et al., 2007, 2008) and the site of "Los Fuegos Eternos" in the Philippines known since the Spanish colonization (Abrajano et al., 1988, 1990). H_2-bearing gases discovered in ophiolitic rocks onshore show lower contents in helium than those discovered in terrestrial context in non-ophiolitic rocks (Coveney et al, 1987; Ikorsky et al., 1999; Sherwood-Lollar et al., 2007; Larin et al., 2015; Zgonnik et al., 2015; Guélard et al., 2017).

H_2 is generally considered as produced by water reduction that occurs simultaneously to the hydration of ultrabasic or basic rocks, *i.e.*, according to serpentinization reactions. In the case of ophiolitic settings, it is generally supposed to happen at low temperature (Moody, 1976;

Neal and Stanger, 1983; Abrajano et al., 1988; Etiope et al., 2011). The process driving this reduction is the change of valence of transition metals, notably ferrous iron Fe^{II} into ferric iron Fe^{III}, iron being the most abundant transition metal in ultrabasic and basic rocks. Fe^{II} is a major component in ultrabasic rocks in the ophiolitic units within minerals such as olivine and pyroxene. It contributes to the formation of Fe^{III}-bearing minerals, such as magnetite. These mineral assemblages are observed in the field, where peridotites are largely serpentinized, mostly along fracture systems. The question of H_2 provenance in oceanic hydrothermal context has been largely approached by petrographic studies and experimental simulations (Allen and Seyfried, 2003; Yoshizaki et al., 2009; Klein et al., 2009; Marcaillou et al. 2011; Neubeck et al. 2011; Shibuya et al., 2015) and numerical modelling (McCollom and Bach, 2009; Klein et al., 2009; Marcaillou et al., 2011). Fe^{II} is initially provided by different minerals (such olivine and pyroxene) in the first stages of hydration, but also by serpentine or ferrous iron hydroxide, which are produced by the alteration processes, thus allowing the H_2 production to go on after olivine and pyroxene have all been transformed (Marcaillou et al., 2011). These studies have shown that depending on thermodynamic conditions, temperature, water chemistry (notably carbonate content, sulphate content and alkalinity), water/rock ratios, different mineral assemblages and sequences are obtained as by-products together with different rates and amounts of H_2. According to the numerical model proposed by McCollom and Bach (2009), the highest rates of H_2 production are obtained at high temperature (about 315°C) while serpentine and magnetite are the main mineral assemblage of the by-products. Onshore H_2-bearing gas seepages yield not only H_2 but also methane and nitrogen, resulting in a three-component gas mixture with proportions varying in a very large range. The origin and the processes of generation of CH_4 and N_2 associated to H_2 are still a matter of discussion in terrestrial ophiolitic units. In the present paper, the geochemical properties of reduced gas seepages from four ophiolite massifs: 1) the Semail ophiolite in the Sultanate of Oman, 2) the Zambales ophiolite in the Philippines, 3) the Antalya ophiolite in southern Turkey and 4) the New Caledonia ophiolite are compared in the light of local geological features to better understand the conditions for di-hydrogen, methane and di-nitrogen production in the geological context of these ophiolite complexes (Fig. 1, 2, 3).

Geological settings

The ophiolitic units in which this study was conducted correspond to wide ophiolitic massifs (Fig. 1) containing rocks which have not been subjected to high pressure-low temperature

(HP-LT) conditions. Peridotites rocks are little serpentinized in wide areas (much less than ophiolites involved in HP-LT conditions). These ophiolites units have been obducted on sediments (Fig. 2) belonging to different paleogeographic domains, either oceanic or continental, which contain, in all cases, clastics and carbonates. The fractures in the peridotite host serpentine and carbonate veins, mainly Mg-bearing carbonates (magnesite, hydromagnesite and dolomite). In the ophiolite-hosted fractured aquifers, groundwater circulations is controlled by fracture hydraulic conductivity. Ultra-basic surface seepages have been found in these ophiolitic massifs and they generally discharge close to the contact between the mantle rocks and overlying former oceanic crust rocks (Moho), and along the basal thrust plane of the ophiolite sequence. This is probably related to favorable drainage conditions in the fractured rocks at the base of the ophiolitic units and to drainage control by the more massive gabbroic units compared to the more fractured peridotites below. They release high pH fluids (commonly higher than 10) which are rich in Ca^{2+}, OH^-, H_2 and CH_4.

More specifically, the Oman ophiolite has been extensively studied, as it is the best large exposed massif of this type in the world (see Hopson *et al.*, 1981; Ceuleneer, 1991; Nicolas *et al.*, 1996, 2000; Python and Ceuleneer, 2003; Arai *et al.*, 2006 and many others). This ophiolite corresponds to parts of the oceanic lithosphere of the Arabian Sea which have been obducted on the Arabian plate during late Cretaceous times. H_2-rich gas seepages associated with Ca^{2+}-OH^--rich groundwater in the Semail ophiolite of Oman were first studied by Neal and Stanger (1983). They proposed that H_2 is the by-product of a low temperature (20-50°C) serpentinization that depends on Fe^{II} hydroxide availability and oxidation by meteoric water that occurs in 2 stages: 1) oxidation by atmospheric O_2 dissolved in meteoric water; 2) oxidation by water. Sano et al. (1993) provided a new insight by analyzing noble gases. Their results confirmed that H_2-rich gas samples are inherited from interaction of meteoric water with Fe^{II} although they propose a high temperature for the reaction (300°C).

In the Philippines, gases were sampled in the Zambales massif, which is located in the north-western part of the Luzon Island (Nicolas and Violette, 1982; Hawkins and Evans, 1983; Abrajano et al., 1988; Yumul et al., 1998; Encarnacion et al., 1999). The gas seepages occur either as bubbling in alkaline springs or seeping out from fractured rocks, locally spontaneously burning as, for instance, in Los Fuegos Eternos and Nagsasa. Gas seepages in the Zambales massif were first studied by Abrajano et al. (1988; 1990). In their paper, they concluded that both mantle origin and serpentinization are consistent with their analytical results and they proposed a temperature of 110-125°C for serpentinization.

The ophiolite of the Antalya region, in southern Turkey, has been extensively studied (Juteau et al., 1977; Robertson and Woodcock, 1980; Glover and Robertson, 1998a, b). Also, the associated sedimentary sequences have been investigated (Bozcu and Yagmurlu, 2001), while oil seepages have also been observed less than 20 km away from the Chimaera site (Hosgörmez *et al.,* 2008). The site of the Chimaera gas seepage has the most spectacular gas outlet since the flames are more intense than those in Zambales, Philippines, and are also more colorful because of a greater content in methane, relatively to the H_2. H_2 seepages associated with the site of the first Olympic fire was first reported by Hosgörmez et al. (2008). From their chemical and isotopic study, they concluded that gas seepages originate from both thermogenic maturation of organic matter and serpentinization. In a later publication, Etiope et al. (2011) confirmed previous conclusions and proposed a temperature lower than 100°C for serpentinization.

The ophiolite of New Caledonia is among the largest onshore massifs of ultrabasic rocks preserved on Earth. The peridotites nappe was emplaced during Eocene times over (1) a basement of arc-derived formations of Pre-Cretaceous age which are overlain by basalts and formations of the Central Range that include sandstones, siltstones, graywackes, claystones with coal of Cretaceous age and Tertiary carbonate turbidites and volcaniclastic deposits, and (2) a tectonic unit of oceanic basalts of Upper Cretaceous to Eocene age, with back-arc or fore-arc affinities which underlies the peridotites nappe (Paris, 1981). H_2-bearing gas seepages associated to alkaline to hyper-alkaline waters were found in the southern part of the Massif du Sud (bay of Prony) within the peridotite nappe (Deville et al., 2010; Monnin et al., 2014; Deville and Prinzhofer, 2016), while N_2-rich seepages were found below the ophiolitic units in the area of La Crouen (Deville and Prinzhofer, 2016).

Materials and methods

Gases were sampled in stainless steel tubes with helium-proof valves for chemical composition and noble gas analyses and in glass tubes for stable isotopic composition analyses. Gas sampling devices were evacuated (10^{-3} Pa vacuum) before sampling. When possible, stainless steel tubes were swept twice by the sampled gas. When gas was collected in water springs, streams or in the sea (Oman, some places in the Philippines and New-Caledonia), pH, Eh and temperature were measured directly in the field (Table 1).

The chemical compositions of gases were determined by gas chromatography (GC) with a Varian GC3800. Measurement uncertainties are below 0.01% mol for hydrocarbons (FID) and

for other gases (TCD). The measurements of the isotopic ratios $^{13}C/^{12}C$ (CH_4 and CO_2) and D/H in (CH_4 and H_2) were performed on a MAT 253 (Thermo Fischer) mass spectrometer coupled with a gas chromatograph (GCC-IR-MS). The results are reported in δ units relative to Pee Dee Belemnite (PDB) for carbon and Standard Mean Ocean Water (SMOW) for hydrogen, respective analytical uncertainties being of 0.5‰ and 5‰. Nitrogen isotopic compositions were measured relative to air with a MAT 253 mass spectrometer. N_2 has been purified in a vacuum line. CH_4 and H_2 were oxidized in a Cu-oxide oven to CO_2 and water vapor, respectively. These produced gases were cryogenically trapped for separation from N_2. Analytical uncertainty for the measurement of $\delta^{15}N$ is lower than 0.1‰.

The noble gases elementary compositions were determined by quadrupole mass spectrometry (Table 2). The QUADRAR line allows determining the contents of ^4He, ^{20}Ne, ^{36}Ar and Kr. The mass spectrometer is a Prisma quadripole QMA/QME200 (Pfeiffer Vacuum) with an open ion source. The analyzer allows measurements of compounds with a mass over charge ratio from 0 to 100. Global relative uncertainties for quantification of noble gases with this method are within the following range: He: ±15%; Ne: ±20%; Ar: ±10%; Kr: ±12%.

Helium isotopic ratios and contents were determined with a high-resolution magnetic sector mass spectrometer Micromass GV 5400 equipped with a modified Nier type electron impact source (Bright). The global relative uncertainty (1σ) on the quantification of ^4He is ±4%. The uncertainty on the quantification of the $^3He/^4He$ ratio is ±2%.

Results

The sites studied in Oman are scattered over Northern Oman and comprise 14 spots of gas bubbling in water (Fig. 1A). Most of the gas samples were taken in ultra-basic springs of the Semail ophiolite and three samples were taken in non-alkaline thermal springs (Rustaq, Nakhal and Al Ali) seeping from formations structurally located below the ophiolite nappe (Table 1). In the Philippines, 3 spots were sampled in the Zambales ophiolite. One site (Mangatarem) corresponds to an ultra-basic thermal spring with abundant bubbling gas, whereas the two others correspond to gas directly seeping from fractures of the peridotites (Table 1). One site corresponds to the Los Fuegos Eternos burning gas close to the Coto Chromite mine (Abrajano et al., 1988, 1990), the other one is located above the Nagsasa bay (Abrajano et al., 2006; Fig. 1B). The gas vents sampled in Turkey were seeping out of the fracture system of the ophiolite unit in the area of Chimaera, south of Antalya (Fig. 1C). In

New Caledonia, all gas samples were bubbling in water (some in alkaline springs of the area of the bay of Prony, others in the non-alkaline thermal springs of the area of La Crouen; Deville and Prinzhofer, 2016; Fig. 1D).

Chemical and isotopic composition of the gas

The gas chemical compositions are listed in Table 1. Gas mixtures contain H_2, N_2 and CH_4 as major components. Figure 4 displays H_2, N_2 and CH_4 molecular contents of all samples in a triangular diagram. Four distinct types of gas mixtures can be identified according to their respective contents in H_2, CH_4 and N_2. Three of these types are associated with water seeps: H_2-rich type; N_2-H_2-CH_4 type and N_2-rich type. The water properties associated to these gas seepages are listed in Table 1 and illustrated on a Pourbaix diagram on figure 5. The last type (H_2-CH_4) corresponds to gas seepages in fractures without associated water flow.

Carbon and hydrogen isotopic composition ($\delta^{13}C$ and δD) of H_2, CH_4, CO_2 and nitrogen isotopic composition ($\delta^{15}N$) of N_2 are reported in Table 2. δD of H_2 values are very negative and comprised in a narrow range from -756 to -699‰, except for the sample from Nagsasa (Philippines) with δD of H_2 = -664‰ (Fig. 6, 7). The highest values of δD of CH_4 correspond to the highest contents of methane (Fig. 8A). Relative carbon and hydrogen isotopic compositions of methane are presented in Figure 8B. High values of $\delta^{13}C$ of CH_4 were obtained, up to +7.9‰, while δD of CH_4 are ranging from -428 to -130‰.

Hydrogen isotopic fractionation between H_2 and CH_4 depends on seepage types. The highest isotopic fractionations between species are observed on dry seepages where δD values of methane are the highest recorded in this study (Table 2). The nitrogen isotopic compositions were also measured for 4 samples. $\delta^{15}N$ values range from -0.3 to +0.5‰ (Table 2).

Noble gases contents and their isotopic ratios, when measured, are given in Table 2. The samples of the H_2-rich type are very close to the air end-member with a slight crustal contribution. Those of the N_2-H_2-CH_4 type show higher N_2 and CH_4 contents and present either a crustal (Oman), or mantle (Kaoris, New Caledonia) or crust plus mantle contribution (Oman). The samples of the H_2-CH_4 type present both crustal and mantle contributions, with a very marked mantle contribution for the Nagsasa sample (Zambales, Philippines). N_2-rich samples are made of a mixing between air and crust end-members.

Gas types

255 According to the gas compositions, four types can be defined (Fig. 4):
256 1) *The H_2-rich type* shows dominant H_2 contents (61.0 to 87.3% mol) associated with some N_2
257 (less than 35% mol) and some CH_4 (less than 20 mol%; Fig. 4 and 8A). This type is
258 encountered in Oman (Neal and Stanger, 1983; Sano et al., 1993; Deville et al., 2010, 2011;
259 Vacquand, 2011; Boulard et al., 2013; Miller et al., 2016) and this type of gas exclusively
260 seeps as bubbles from ultra-basic springs (pH between 11 and 12; Fig. 5) associated to
261 negative to very negative Eh (from -45 to -780 mV; Fig. 5; table 1). In addition to the high
262 OH^- ion concentration responsible for the high pH, the waters are calcium-rich (Neal and
263 Stanger, 1985). Consequently, in the alkaline springs, spectacular precipitations of calcium
264 carbonate (calcite and aragonite) are observed due to the reaction of Ca^{2+} and OH^- ions with
265 the CO_2 of the atmosphere (see supplementary material). These waters show high electrical
266 conductivities in accordance with their relatively high salinity, essentially related to the
267 presence of Cl^- and Na^+ ions (Cl^- between 120 and 380 mg/l; Na^+ between 150 and 420 mg/l;
268 Neal and Stanger, 1985; Kelemen et al., 2011). The temperatures of these sources are almost
269 ambient to slightly warm (between 22.5 and 35 °C). The $\delta^{13}C$ values of methane are very high
270 (among the highest values known on Earth, between -13 and +8‰; Table 2; Fig. 8B). The gas
271 composition shows N_2 *vs* fossil noble gas ^{36}Ar ratios (Table 2; Fig. 9) comprised between the
272 air and water in equilibrium with air (classically mentioned as ASW for Air Saturated Water).
273
274 2) *The N_2-H_2-CH_4 type* is characterized, by higher N_2 values (from 45 to 65 mol%) compared
275 to the previous gas type. Therefore N_2 becomes the main gas. H_2 contents range from 25 to 36
276 mol%. CH_4 concentrations are similar to those of the H_2-rich type (below 20 mol%; Fig. 4).
277 This second gas type is mainly found in New Caledonia (Deville and Prinzhofer, 2016) but
278 also in some springs of Oman and of the Philippines. This type of gas mixture seeps also in
279 ultra-basic springs. These springs are generally warmer than those of the H_2-rich type, up to
280 40.1°C in New Caledonia and pH values are slightly lower, ranging from 10.5 to 11.3. They
281 are, as well, associated with precipitations of calcium carbonate (see supplementary material).
282 The $N_2/^{36}Ar$ ratios of this gas type are different from the previous type and higher than those
283 recorded for ASW and air (Table 2; Fig. 9). These ratios are also correlated with $H_2/^{36}Ar$ and
284 $^4He/^{36}Ar$ ratios (Deville and Prinzhofer, 2016). $\delta^{13}C$ of methane recorded for this gas type
285 ranges between -38.5 and -32.4‰ (Deville and Prinzhofer, 2016).
286

287 3) *In the N_2-rich type,* the dominant gas compound is N_2 (over 91 mol%). Gas mixture is H_2-
288 free with low CH_4 contents (up to 2.7 mol% in New Caledonia), plus substantial amounts of
289 helium (values above 0.1 mol%). This type of springs was found in Oman (Sano et al., 1993;
290 Vacquand, 2011) and New Caledonia (Deville and Prinzhofer, 2016) where they occur in the
291 same structural position, *i.e.*, at the base of ophiolitic nappes (either in the sole of the nappes
292 or in the sediments immediately below the nappes). $\delta^{13}C$ values of CH_4 in this type are
293 between -39.2 and -12.1‰. These gases come out in the form of bubbling springs with less
294 alkaline water than previously recorded (pH from 7.5 to 10) and variable Eh (from -230 to
295 +146 mV). The $N_2/^{36}Ar$ ratios are very high (Table 2; Fig. 9). R/Ra ratios of the gases are
296 consistently low (between 0.06 and 0.08, except for the sample collected in Al Ali where it
297 was not possible to avoid air contamination because of access difficulties when sampling the
298 gas and high temperature of the spring, above 66°C; Tables 1 and 2; Fig. 10). The dissolved
299 species in the associated waters are very different from those of the waters containing H_2
300 gases. They show lower concentrations of Na^+ and K^+ ions and contain HCO_3^- ions, which is
301 not the case of the ultra-basic springs with H_2 seepages (Neal and Stanger, 1985). In all cases
302 these springs are warm to hot (from 37.9 to above 66°C; Table 1).
303
304 4) *The H_2-CH_4 type* shows mostly H_2 and CH_4 in variable proportions. This type of gas vent is
305 characterized by focused and relatively high gas flows (> 1 l/s), coming directly out of the
306 rock fractures in the absence of water. This gas type was found in the Philippines and in
307 Turkey where it was mentioned respectively by Abrajano et al. (1988; 2006) and Hosgörmez
308 et al. (2008). It has not been found in New Caledonia but Neal and Stanger (1983) mentioned
309 locally focused high gas flows seeping out directly from fractures of ultrabasic rocks in Oman
310 (> 10 l/s). The CH_4/H_2 ratio is commonly higher compared to the types associated to alkaline
311 springs, except for the case of Nagsasa in the Philippines. The gas is able locally to
312 spontaneously ignite as it is the case in Turkey (Chimaera) and the Philippines (Los Fuegos
313 Eternos and Nagsasa) forming visible flames when the CH_4/H_2 ratio is high. Nitrogen is
314 nearly absent of these dry gas seepages (less than 2 mol%; Fig. 4) whereas since the gas is
315 seeping out from fractures of rocks located above the water table, we would have expected
316 that the gas would be much more easily naturally contaminated by air than in the previous
317 cases which are bubbling in water. Indeed, these H_2-CH_4 gases do not display predominantly
318 atmospheric features and ^{20}Ne and ^{84}Kr concentrations are quite low compared to other types
319 of gas mixtures (Table 2). $\delta^{13}C$ values of CH_4 are high and fairly constant (between -12 and -

5‰; Fig. 8), as well as δD of CH_4 which range from -175 to -130‰. The δD values of CH_4 are higher when compared to the H_2-rich and N_2-H_2-CH_4 gas types (Table 1), while the δD values of H_2 vary between -756 and -664‰, generally in the same order of magnitude as those recorded in the H_2-rich and N_2-H_2-CH_4 gas types (Table 1; Fig. 6). The differences of δD values of CH_4 suggest different processes for CH_4 genesis and probably different sources for hydrogen and carbon (see discussion below).

Discussion

Main characteristics of the different gas types

Comparing the different gas types, several characteristic features can be noticed. Gases bubbling in prings always contain N_2 that is not related to air contamination (see below), while gas seepages in fractures without associated water flows are N_2-poor. The gas bubbling in springs show CH_4 contents that never exceed 20 mol%. The specificity of the H_2-CH_4 gas type seeping in fractures without associated water flow is that their CH_4 contents locally reach high levels and that δD of CH_4 is significantly higher compared to the δD of CH_4 in the other gas types (Fig. 8). The water temperature tends to increase in the different types of springs from the H_2-rich, to the N_2-H_2-CH_4 and to the N_2-rich gas types (Table 1). Gas bubbling in springs is associated to ultra-basic conditions only when H_2 is present, whereas water is less or not basic in the springs of the N_2-rich gas type. We propose that the chemical characteristics that define gas types reflect differences in origin and transport pathways of gas mixtures.

Hydrogen origin

As mentioned in introduction, H_2 sources of gas seepages in ophiolitic contexts are classically credited to modern hydration processes at low temperature during the weathering of ultrabasic and basic rocks (mostly peridotite and gabbro). At depth, within ophiolitic rocks, biological production of H_2 by fermentation processes is probably a sluggish process due to the paucity of potential organic substrates. High-temperature serpentinization (above 300°C) is a well-known process but at temperatures below 300°C serpentinization can occur as well (Moody 1976). Indeed, experimental studies simulating land-based peridotite systems have shown that

353 H_2 can be generated during serpentinization at temperatures below 100°C (Mayhew et al.,
354 2013; Okland et al., 2014; Neubeck et al., 2011). On hydrogen-bearing gas seepages
355 associated with high pH waters in ophiolitic context (Neal and Stanger 1983; Sano *et al.*
356 1993; Cipolli *et al.* 2004; Hosgörmez *et al.* 2008; Abrajano *et al.*, 2006; Vacquand, 2011), H_2
357 would result from the interaction between ultrabasic rocks and water flows at depth in the
358 fracture system, in anoxic conditions, by reduction of water and oxidation of metals (Fe^{II},
359 Mn^{II}, Ni^{II}…), Fe^{II} being by far the most abundant electron donor in ultrabasic-basic rocks.
360 During the serpentinization process, Fe^{II}-rich minerals, such as olivine [$(Mg^{II},Fe^{II})_2SiO_4$] are
361 oxided and form Fe^{III}-bearing minerals, such as magnetite [$Fe_2^{III}Fe^{II}O_4$] or Fe^{III}-bearing
362 serpentine (Evans et al., 2008), with coeval reduction of water generating H_2. Olivine is a
363 magnesium-iron nesosilicate forming a solid solution series between a Mg-endmember and a
364 Fe- endmember. During olivine dissolution, the olivine Fe-endmember (fayalite, Fe_2SiO_4)
365 tends to react as,
366
367 $$3\ Fe_2SiO_4 + 2\ H_2O \rightarrow 2\ Fe_3O_4 + 3\ SiO_2 + 2H_2 \quad (1)$$
368 *Fayalite + water → Magnetite + silica + dihydrogen*
369
370 At temperature below 150°C, dissolution of the olivine Fe-endmember is even
371 thermodynamically more favorable when Fe-chrysotile is formed (Oze and Sharma, 2005)
372 according to the following reaction,
373
374 $$6\ Fe_2SiO_4 + 7\ H_2O \rightarrow 3\ Fe_3Si_2O_5(OH)_4 + Fe_3O_4 + H_2 \quad (2)$$
375 *Fayalite + water → Fe-Chrysotile + Magnetite + dihydrogen*
376
377 The Mg-endmember of olivine (Forsterite, Mg_2SiO_4) reacts as,
378
379 $$2\ Mg_2SiO_4 + 3\ H_2O \rightarrow Mg_3Si_2O_5(OH)_4 + Mg^{2+} + 2OH^- \quad (3)$$
380 *Forsterite + water → Chrysotile + magnesium ions +hydroxyl ions*
381
382 In presence of dissolved inorganic carbon (DIC) in subsurface, Mg^{2+} ions are consumed to
383 produce magnesium-bearing carbonates (which are widespread in fractures systems of all the
384 ophiolitic massifs studied here; see below), and (if available) remaining Mg^{2+} ions are prone
385 to react with OH^- to form brucite, $Mg(OH)_2$ (which is commonly found in the ultra-basic
386 springs studied here, notably in Oman; Neal and Stanger, 1984) leaving finally OH^- available

in solution. In the case of New Caledonia, where alkaline seepages interact with sea water, this results in massive production of brucite due to the reaction between OH^- and Mg^{2+}present in sea water as it is the case of the seepages studied in New-Caledonia (Launay and Fontes, 1985). More generally, as proposed by different authors, the coupled hydration of Mg-olivine and Ca-bearing pyroxene of peridotite rocks makes the water enriched in Ca^{2+} and OH^- (Barnes et al., 1967; Neal and Stanger, 1984; Bruni et al., 2002; Kelemen et al., 2011; Miller et al., 2016),

$$4\ Mg_2SiO_4 + CaMgSi_2O_6 + 7H_2O \rightarrow 3\ Mg_3Si_2O_5(OH)_4 + Ca^{2+} + 2OH^- \quad (4)$$

Forsterite + Clinopyroxene + water → Serpentine + calcium ions +hydroxyl ions

As such, the interaction between peridotite and water during serpentinization is a potential source of H_2 caused by ferrous iron oxidation and water reduction associated with a rise of pH due to OH^- production and associated with the presence of Ca^{2+} in the ultra-basic water. The richer in iron is the olivine, the more H_2 and the less OH^- are produced.

It has been experimentally demonstrated that highly fractured/altered peridotite is more prone to generate H_2 than a massive unaltered peridotite suggesting a role of the reacting surfaces and possibly that Fe^{II}-bearing secondary formed minerals, such as Fe^{II}-bearing brucite and serpentine, and the presence of N-species may also contribute to form H_2 (experiments at 25°C; Okland et al., 2014, see also Klein et al., 2015).

The conditions of generation of H_2 can be estimated notably using hydrogen isotopic data. In the studied ophiolitic massifs, whatever are the characteristics of the H_2-bearing gas types, δD values of H_2 are all very low in the analyzed gas samples (between -756 and –664‰). Abrajano (1988) mentioned , δD values of H_2 at -581 and -599‰ in the Los Fuegos Eternos of the Philippines. The lowest values are among the lowest recorded on Earth and they are significantly lower compared to δD of H_2 of hydrothermal sites on mid-oceanic ridges for which the values are more dispersed and generally higher (between -700 and -300‰; Fig. 6). δD values of H_2 observed in oceanic settings decrease with temperature and appear as a thermometer for H_2 production at isotopic equilibrium with seawater (Proskurowski et al., 2006). Low δD values of H_2 in ophiolitic massifs are classically considered as revealing relatively low temperatures of the generation of H_2 (Neal & Stanger 1983). Indeed, using either (1) the Horibe and Craig (1995) H_2O–H_2 and CH_4–H_2 geothermometers which consider isotope fractionations between liquid H_2O or CH_4 and H_2, or (2) Bottinga's 1969 water vapor–hydrogen method, this strongly suggests that the generation of H_2 occurred at lower

421 temperature conditions than at most of the hydrothermal vents of mid-oceanic ridges. H_2O–H_2
422 is seen as the preferred geothermometer but it implies that chemical equilibrium between H_2
423 and H_2O has been reached (see discussion below). It is possible that chemical and isotopic
424 equilibrium have been achieved between H_2 and CH_4 (see the following paragraph). Whatever
425 the geothermometer used, either the Horibe and Craig (1995; Fig. 7) H_2O-H_2 and CH_4-H_2
426 geothermometers, or the Bottinga (1969) geothermometer, we obtained relatively narrow
427 windows of temperature conditions in the ranges 17 to 42°C for H_2 of the H_2-rich type and
428 24-50°C for H_2 of the N_2-H_2-CH_4 gas type, whereas the temperature conditions seem much
429 more heterogeneous and reach much higher temperatures in the H_2-CH_4 gas type, notably for
430 the samples of the Philippines (up to 136°C, taking into account the δD_{H2} values from
431 Abrajano et al., 1988).
432 To decipher the conditions of generation of H_2, it is possible to compare H_2 contents with
433 those of other compounds such as noble gases tracers (Ballentine et al., 2002a and b; Zhou et
434 al., 2005; Burnard et al., 2013; Prinzhofer, 2013; Prinzhofer and Deville, 2013). Notably, the
435 H_2-rich gas type displays $N_2/^{36}Ar$ ratios between ASW and air (Table 2; Fig. 9). These
436 features are consistent with a genesis process involving surface water charged with dissolved
437 atmospheric components (ASW) as the main fluid reacting with the rock for H_2 production. In
438 this case, H_2O inherited from meteoric water, initially in equilibrium with atmospheric
439 components, is probably consumed at depth in the fracture system of the ophiolites by
440 water/mineral interactions. Following this interpretation, as a consequence of water
441 consumption and H_2 production, initial gas/water equilibrium with atmosphere is disrupted
442 and atmospheric nitrogen and noble gases are mixed with neo-formed gases (H_2 and CH_4) and
443 migrate upwards with no further addition of another gas component. The preservation of
444 atmospheric relative proportions of fossil noble gases (^{20}Ne, ^{36}Ar, ^{84}Kr) suggests that these
445 groundwaters reacted at a relatively shallow depth. For deeper depths of gas/water phases
446 interaction, the difference of noble gas solubility from the surface conditions' ones (as P and
447 T are much higher) would fractionate the relative proportions of these compounds. The ^4He
448 contents (< 20 ppm), are in good agreement with Neal and Stanger's (1985) interpretation
449 which asserts that Ca^{2+}-OH^- water originates from meteoric water recharging at high
450 elevations. The presence of ^4He in subsurface gas is classically interpreted as the result of a
451 lengthy residence time at depth allowing ^4He to accumulate significantly due to natural
452 radioactive decay of ^{235}U, ^{238}U and ^{232}Th present in crustal rocks (Ballentine and Burnard, 2002).
453 Paukert et al. (2012) considered, from their modelling of CO_2 consumption, that such
454 meteoric waters reached its high pH values after 6500 years. This geological short time frame

455 is consistent with the low ^{4}He contents of these gases, which are roughly displaying
456 atmospheric signatures.
457 Considering the N_2-H_2-CH_4 and H_2-CH_4 gas types, the interpretation that H_2 generation is
458 simply a result of interaction between meteoric water and ophiolitic rocks is not sustainable
459 anymore because, notably, $N_2/^{36}Ar$ ratios are not comprised between ASW and air and noble
460 gas contents are different from Air or ASW. This is consistent with a H_2 generation process
461 which occurred deeper than in the H_2-rich gas type, in higher temperature conditions as
462 already suggested by δD values of H_2.
463
464 *Methane origin*
465
466 Methane generation associated with fluid-rock interaction in ophiolitic contexts remains
467 unclear. In terrestrial ultrabasic-basic contexts at moderate temperatures (below 150°C),
468 methane is interpreted to result from carbon hydrogenation involving mainly sources of
469 inorganic carbon. Methane so formed is termed abiotic (or abiogenic), and is thought to be
470 produced by chemical reactions that do not directly involve organic matter (see discussion in
471 Etiope and Sherwood Lollar, 2013; with references therein). Eventually, according to the
472 geological conditions, methane produced by fluid-rock interaction can be mixed with biotic
473 methane produced either by microbial processes or by thermogenic degradation of organic
474 matter in sedimentary rocks.
475 In the case of hydrogenation processes of carbon, considering potential hydrogen sources
476 (H_2O or H_2), hydrogen in CH_4 can be considered as primary (*i.e.*, issued from H_2O reacting
477 with carbon and preceding H_2 production; Abrajano et al., 1988; Oze and Sharma, 2005; Suda
478 et al. 2014; Okland et al., 2014), or secondary (i.e., issued from an H_2 intermediate by
479 reactions between carbon and H_2; Berndt et al., 1996; Foustoukos and Seyfried, 2004: Horita
480 and Berndt, 1999; McCollom and Seewald, 2001; McCollom, 2016; Neubeck et al., 2011).
481 The experiments of Okland et al. (2014) suggest indeed a possible primary production of CH_4
482 during hydration of ultrabasic rocks without an H_2 intermediate, notably with moderately
483 altered peridotites. In both cases, hydrogen is issued from H_2O, either primarily or
484 secondarily. Suda et al. (2014), based on a study of hydrogen isotopic data of CH_4, H_2 and
485 H_2O (Fig. 7), defined different domains corresponding to different processes allowing to
486 distinguish CH_4 generation by hydrogenation from water (primary) or from H_2 (secondary).
487 Primary CH_4 production is regarded as a direct interaction between Fe^{II}-rich minerals and

dissolved CO_2. CH_4 production tied to ferrous mineral reactions with CO_2 has not yet been fully explored (Neubeck et al., 2016) but there is some indication from experimental reactions of olivine that passivating layers of silica may coat reactive surfaces and slow related CH_4 generation (Garcia et al., 2010). However, early production of CH_4 (before H_2 production) has been documented by experimentation on natural peridotite rocks, at low temperature (25°C), especially on fractured and altered peridotite, and these experiments showed a coeval production of H_2 and CH_4 (Okland et al., 2014), in the same proportions as those measured in this study for the H_2-rich gas type. The presence of CO_2 is a favorable factor for olivine dissolution (Oze and Sharma, 2005), which releases aqueous Fe^{II}. Primary production of CH_4 from H_2O and CO_2 (DIC in water) is achieved in a similar way as the H_2 production through the oxidation of iron (see above). The reaction of the Fe-endmember of olivine in presence of dissolved CO_2 can be summarized by the following reaction,

$$6\ Fe_2SiO_4 + 2\ H_2O + CO_2 \rightarrow 4\ Fe_3O_4 + 6\ SiO_2 + CH_4 \quad (5)$$

Fayalite + water + carbon dioxide → Magnetite + silica + methane

while a coeval reaction occurs considering the Mg-endmember,

$$2\ Mg_2SiO_4 + 2\ H_2O + CO_2 \rightarrow Mg_3Si_2O_5(OH)_4 + MgCO_3 \quad (6)$$

Forsterite + water + carbon dioxide → Serpentine + magnesite

Over geologic time, in natural environments that include fractured and weathered ultrabasic rocks experiencing diverse aqueous geochemical conditions, passivating silica layers may not be widespread allowing the folling reaction,.

$$3\ Mg_2SiO_4 + 4\ H_2O + SiO_2 \rightarrow 2\ Mg_3Si_2O_5(OH)_4 \quad (7)$$

Forsterite + water + silica → Serpentine

Also, Fe^{II}-bearing brucite-type minerals (for example amakinite) and Fe^{II}-bearing serpentines are also good candidates to react with dissolved CO_2, as suggested by experiments (Okland et al., 2014).

Applying the reasoning of Suda et al. (2014) mentioned above to our samples, would suggest that gases from the H_2-CH_4 type (dry seepages in fractures) contain methane which is considered as primary while, in water-related seepages, the analytical results are more

compatible with a secondary CH_4 generated from an H_2 intermediate (gas samples collected in ultra-basic springs showing δD values of CH_4 between -400 et -200‰; Fig. 7).

As suggested by Suda et al. (2014) and according to the reactions shown above, a simultaneous production of methane and magnesite can occur. Mg-bearing carbonates (magnesite and dolomite) are indeed abundant in fractures in the peridotites of Oman and they are supposed to have been formed at temperatures in the range 30 to 60°C (Kelemen et al., 2011). Methane and magnesite, have both high and similar $\delta^{13}C$ values ($\delta^{13}C_{CH4}$ between -13 and +8‰, $\delta^{13}C_{magnesite}$ between +2 and +8‰; see supplementary material). This is compatible with a non-atmospheric carbon origin of CH_4 that could derive from mantellic or metamorphic CO_2 or from carbonate destabilization. These values are different from the carbonates signatures found at the surface in the ultra-basic springs where carbon is interpreted as issued from atmospheric CO_2 which after fractionation during carbonate precipitation give $\delta^{13}C$ values between -28 and -5‰ (Kelemen et al., 2011; see also supplementary material).

Considering secondary production of methane, via an H_2 intermediate, several pathways of CH_4 generation involving different sources of carbon can be considered, either (1) organic carbon (or reduced carbon including elementary C) found in sediments below the ophiolites notably, or else (2) carbon issued from deep sources from the mantle or from the crust (for example Dissolved Inorganic Carbon issued mantle gas or from carbonates within the sediments). Indeed, H_2 produced by serpentinization is susceptible to be subsequently consumed in a CH_4 producing reaction, involving a source of carbon which can be C°, CO or CO_2, according to the general reaction (Deville and Prinzhofer, 2016),

$$(2 + x)\ H_2 + CO_x \rightarrow CH_4 + x\ H_2O \qquad (8)$$

In the case $x = 0$, the source of carbon can correspond to reduced carbon in sediments (graphite or overmature organic matter). In the case $x = 1$, the source of carbon corresponds to CO. CO has indeed, been mentioned as traces in the gas of the ophiolites of Oman (Sano et al., 1993). It might correspond to an intermediate compound preceding methane generation. In the case $x = 2$, this corresponds to the classical Sabatier reaction. Considering generation of high $\delta^{13}C$ methane associated with ultrabasic contexts, it is frequently considered that it corresponds to Fisher-Tropsch Type (FTT) reaction, meaning the abiotic path of the Sabatier reaction (Szatmari, 1989; Horita and Berndt, 1999; Sherwood-Lollar et al., 1988, 1993a&b, 2006, 2007; Kelley et al., 2001; Charlou et al., 2002; Foustoukos and Seyfried, 2004;

McCollom and Seewald, 2006; Taran et al., 2007; Proskurowski et al., 2008; and others, see references in Etiope and Sherwood-Lollar, 2013). In the Sabatier reaction, CO_2 is reduced to CH_4 through the oxidation of H_2 (so the reaction is controlled by H_2 activity).

The kinetics of FTT reactions are slow at the temperatures considered here (below 150°C) but Fisher-Tropsch reactions are well-known to be favored by catalytic processes. Heterogeneous catalysis, promoted by minerals present in the ophiolitic rocks, such as chromite, magnetite, sulfides or awaruite can possibly trigger these reactions (Mayhew, 2013; Etiope and Ionescu, 2015 and references therein). For instance, close to Los Fuegos Eternos (in the Philippines), chromite (well-developed in the Coto mines) may promote the catalytic production of CH_4. Also, the area of Chimaera in Turkey shows chromite mines (in which an explosion caused the death of tens of underground workers). The area of Prony (New Caledonia) shows also chromite outcrops as well as at many places in the ophiolite of Oman.

Catalytic processes might also be associated with biological activity, which is well-known to reduce the activation energy necessary for chemical reactions. The Sabatier chemical reaction is actually equivalent to one of the classical routes to generate microbial methane (by CO_2 reduction) via hydrogenotroph-methanogen microorganisms. In the case of sedimentary environment with widely available sources of light C provided by organic compounds, it produces methane with $\delta^{13}C$ generally lower than -50‰, far below the values obtained in the gas seepages of the ultra-basic springs (between -12.8 and +7.9‰; Fig. 8), even if locally in ultra-basic springs $\delta^{13}C$ of methane are lower than -50‰ (Morrill et al., 2013). However, in some conditions (notably in the case of hyperthermophilic archaea), $\delta^{13}C$ values of methane can be high (Takai et al., 2004, 2008). The presence of hydrogenotrophic microorganisms has been mentioned in oceanic hydrothermal fields (Bradley and Summons, 2010) and in ultra-basic springs of ophiolitic units (Brazelton et al., 2013), and the occurrence of methanogens in ultrabasic contexts (Takai et al., 2004; Brazelton et al., 2006) raise the question, notably in Oman, of the microbial production of methane with elevated $\delta^{13}C$ in ultra-basic groundwaters (Miller et al., 2016). This interpretation is still challenged (see discussion between Etiope, 2017 and Miller et al., 2017) but, if it is confirmed, this would suppose that biological activity might contribute to elevated $\delta^{13}C$ methane from inorganic sources of carbon under extreme carbon limitation. However, methanogens collected in ultra-basic springs at the surface are not necessary representative of the conditions of generation of methane at depth because there is no carbon available in the ultra-basic water flowing from depth (Neal and Stanger, 1985, see also below). Methane generation via methanogen microorganisms observed at the surface

might be a surficial process resulting from a a reaction between hydrogen issued from depth and a source of carbon provided by atmospheric CO_2. If the source of deep carbon is important, as in sedimentary environments with fossil organic matter, the use of isotopically light carbon in the widely available organic matter is favored by microbial activity. However, this is not possible in the case of strong restriction of the available carbon as in ophiolitic rocks, especially when the initial sources of carbon are heavy (like carbonates or mantle). Biological processes generating CH_4 from H_2 and CO_2 with progressively increasing $\delta^{13}C_{CH4}$ have been documented in large scale geological gas storages of town gas (Buzek et al., 1994). In addition, the presence of methanotrophs in the ultra-basic springs also contribute to increase the $\delta^{13}C$ values of the residual methane (Miller et al., 2016).

In the present study, the different values observed for $\delta^{13}C$ of CH_4 probably reflect different sources of carbon or different CH_4 generation processes. The present study shows that (a) H_2-rich gases from Oman display $\delta^{13}C$ of CH_4 between -12.8 and +7.9‰, while (b) in the Philippines $\delta^{13}C$ of CH_4 are ranging between -13.5 and -5.6‰ which is compatible with the results obtained by Abrajano et al. (1988), (c) in Turkey gases from H_2-CH_4 type display a $\delta^{13}C$ of CH_4 values between -7.9 and -11.9‰ (Horgormez et al., 2008 and this study), whereas (d) for New-Caledonia some gases from N_2-H_2-CH_4 type values are between -38.5 and -32.4‰ (Deville and Prinzhofer, 2016). Consequently, two different types of signatures were observed corresponding initial probably (despite of fractionation processes) to two different carbon sources. The first one (high $\delta^{13}C$ between -13 and +8‰) would correspond most probably to an inorganic carbon source, while the second one (lower $\delta^{13}C$ between -39 and -32‰) corresponds probably to an organic source. The high $\delta^{13}C$ of CH_4 from Oman, the Philippines and Turkey might correspond to a carbon source, probably CO_2, found as DIC in the reacting waters. Two different origins may be proposed for this inorganic carbon. It may correspond to mantle degassing, as it might be the case in the Philippines in link with the vicinity of the active volcanism of the Pinatubo system related to an active subduction zone, as suggested by noble gas analyses especially for one gas sample with high R/Ra values (Fig. 10), or it may come from the dissolution of carbonate rocks (for instance the carbonate sediments present under the ophiolites), as it might be the case in Oman (Nicolas et al., 2000) and Turkey (Juteau et al., 1977). Note that the H_2-bearing gas samples studied here (as well as those analyzed in previous studies) show only locally tiny traces of CO_2 for which $\delta^{13}C_{CO2}$ measurements have to be considered with caution (not reported in table 2). The measurements in the N_2-rich gas type of Oman (seeping out from below the ophiolites), in which CO_2

contents are more important (data from Sano et al., 1993, and this study, Table 1 and 2), gave values between -19.4‰ and -9.6‰ which are consistent with an origin from sedimentary rocks below the ophiolites (metamorphism and/or carbonate destabilization).

Methane with $\delta^{13}C$ values comprised between -39 and -32‰, in New Caledonia, could simply be issued from an organic source (Deville and Prinzhofer, 2016). In agreement with the absence or low contents of C_{2+} in the gas mixtures (below 0.01%), methane may originate from a reaction between H_2 and a mature/overmature organic matter or graphite present in the sediments below the ophiolites.

Also note that, in addition to the absence or very low contents of CO_2 in H_2-bearing gas samples, neither HCO_3^- nor CO_3^{2-} have been found in the ultra-basic springs, notably in the case of Oman (Neal and Stanger, 1985) suggesting that almost the entire stock of available DIC was converted into CH_4 under extreme carbon limitation. Also, no form of organic matter or graphite are known within the peridotites of the areas studied. This limitation probably allows H_2 to be present in the gas, otherwise all the generated H_2 would have been consumed to generate CH_4, as it was suggested by Milesi et al. (2016) in the Solimes Basin in Brazil.

In both, H_2-rich and N_2-H_2-CH_4 gas types, CH_4 contents being lower than 20 mol%, this suggests a very limited carbon source compared with the H_2-CH_4 gas type (Fig. 4 and 8). Indeed, if we consider carbonic acid in rain water as the initial main source of carbon, its contribution is regarded as limited and rapidly buffered, whereas if the carbon source corresponds to carbonate rocks or deep CO_2 fluxes, the amount of carbon available is more abundant at depth but the connection with the ophiolites depends on the hydrodynamics and the available carbonate dissolved in circulating water. H_2-CH_4 gas type might correspond to such a system connected to deep sources of carbon.

Considering oceanic hydrothermal vents, values of δD of CH_4 probably record the isotopic fractionation associated to a primary process involving a carbon compound with water, to produce methane. If open system conditions apply, δD of CH_4 depends on isotopic equilibrium at the given temperature. For dry seepages in fractures, data are in agreement with these conditions. For seepages in water, a different process would provide scattered and very low δD values of CH_4 (Fig. 6), either because the system is closed and isotopic equilibrium is not reached or because a different secondary process (eventually biology) is influencing the isotopic composition of hydrogen in methane. As such, the very low values of δD of methane in spring water raise the question of a possible microbial role in methane generation.

For the H_2-CH_4 and N_2-H_2-CH_4 gas types a remarkable correlation exists between H_2 and CH_4 when normalized to ^{36}Ar (Fig. 11A) wherever is the site studied in Oman, in the Philippines and New Caledonia. A similar correlation exists between H_2 and CH_4 when normalized to ^{84}Kr, (Fig. 11B). For the CH_4-H_2 and N_2-H_2-CH_4 gas types, this suggests that, independently of the considered ophiolite and geological context, generations of H_2 and CH_4 are coupled and both related to a deep process which is independent of interactions with ASW shallow aquifers. Conversely, these correlations do not exist for the H_2-rich gas type which is in agreement with the interpretations proposed above that this type of gas underwent more influences with ASW aquifers. Also, this correlation is not observed in the samples of Turkey possibly due to a mixing with thermogenic methane. Indeed, according to other studies, some samples, notably in Turkey (H_2-CH_4 type), might comprise a thermogenic component. It has been considered that high methane content cannot be attributed univocally to dissolved carbonates reduction by H_2, for example in Chimaera (Turkey), up to 40 mol% of the CH_4 has been estimated to be thermogenic gas originating from a source rocks with highly mature kerogen in a Mesozoic limestone nearby (Hosgörmez et al., 2008; Etiope et al., 2011). This is in good agreement with occurrences of C2+ (C_2–C_6 alkanes) in the gas analyzed in Turkey (Hosgörmez et al., 2008; Etiope et al., 2011, and this study, see table 2). However, whatever the geographic location of samples is, dry seepages display higher CH_4 relative contents together with higher δD of CH_4 when compared to gas seepages in water. This suggests that it can be linked to a different process as mentioned above (primary methane production) and probably higher temperature during production of methane. Gas mixtures belonging to the H_2-CH_4 type correspond probably to highly reactive zones of water reduction at higher temperature with less carbon restriction.

Nitrogen origin

In the subsurface, nitrogen gas can have different origins, either atmosphere via the hydrodynamism of air equilibrated water, or sediments (organic matter, or ammonium-bearing clay minerals, or nitrogen-bearing salt in evaporites present in sedimentary rocks), or else the deep crust or mantle degassing (Jenden et al., 1988; Zhu et al., 2000; Ballentine and Sherwood-Lollar, 2002b). Nitrogen contents within ophiolitic rocks are low but experimental studies have however shown that adsorbed N-species can be leached out while H_2 and CH_4 are produced from altered peridotites (Okland et al., 2014).

686 Considering the geochemical results of this study, N_2 present in the gas of the H_2-rich type
687 shows $N_2/^{36}Ar$ and $N_2/^{84}Kr$ ratios generally equivalent or slightly higher than those of ASW,
688 suggesting mainly an atmosphere origin for N_2 via a fractured aquifer (Fig. 12A and B).
689 Samples of the N_2-H_2-CH_4 gas type, which show higher N_2 contents than H_2 contents
690 compared to the H_2-rich gas type display notably a nitrogen enrichment relative to ^{36}Ar and
691 ^{84}Kr (Fig. 12A and B), suggesting an addition of non-atmospheric nitrogen. This contributes
692 to dilute the neo-formed H_2 and CH_4 (Deville and Prinzhofer, 2016). Samples of the N_2-rich
693 gas type show a ^4He enrichment correlated with the N_2 enrichment when compared to
694 atmosphere (Fig. 13). This suggests that non-atmospheric N_2 might be of crustal origin
695 associated to radiogenic helium from depth. The R/Ra ratio ($^3He/^4He$ ratio of the sample
696 normalized over the same ratio for the air = 1.384×10^{-6}) suggests that a crustal component
697 exists in most of the samples and locally a mantle component is observed in the Philippines
698 (Fig. 10).
699 The differences between the H_2-rich type and the N_2-H_2-CH_4 type are possibly linked to the
700 existence of two different reactive zones for the production of H_2-rich fluids in peridotitic
701 ground waters: one (H_2-rich) being more surficial than the other (N_2-H_2-CH_4-rich) and that
702 two different reactive fluids should be considered: (1) a meteoric fluid in the more surficial
703 environment (H_2-rich) and (2) a deep N_2-bearing fluid with crustal signature, probably issued
704 from sediment metamorphism from below the obducted ophiolitic units.
705 Samples of the N_2-H_2-CH_4 type could also result from the mixing of H_2-rich gas and N_2-rich
706 gas. These N_2-rich samples contain mostly N_2 and no or little H_2. Because they were found in
707 hot water springs, displaying pH between 6.9 and 10 and relatively high ^4He contents which
708 suggest a different origin, probably deeper according to water temperature (reaching locally
709 66°C) and in a crustal environments as suggested by the high ^4He contents. This deep N_2 is
710 probably not directly produced within the peridotite units. The geological context suggests
711 rather an origin from the underthrusted sediments below the ophiolitic units, so in this case N_2
712 would be issued more probably from the buried sediments, either from the water of hydrated
713 clay (clay dewatering) or from the destabilization of ammonium-bearing clays. Reaction of
714 such deep fluids with peridotite or mixing these fluids with H_2-rich gas type are susceptible to
715 generate fluids with the chemical signatures of the N_2-H_2-CH_4 gas type where N_2 dilutes H_2
716 and is found in excess relative to ASW or air. Throughout the study of the 4 types of gas, it
717 appears that the presence of nitrogen in the mixture is always linked to the presence of water
718 at the seepage. This gas is almost absent from the dry seepages (H_2-CH_4 type).

719 $\delta^{15}N$ measurements in the nitrogen-dominant gas types (N_2-H_2-CH_4 and N_2-rich), gave values
720 of -0.3‰ in Rustaq (Oman), which is consistent with previous studies (Sano et al, 1993) and -
721 0.1‰ in Mangatarem (Philippines; table 2), whereas $\delta^{15}N$ measurements in the H_2-CH_4 gas
722 type gave values comprised between -2.8‰ and -2.1‰ in the Chimaera gas seepages of
723 Turkey (Hosgörmez et al., 2008) and +0.5‰ in Nagsasa in the Philippines (Table 2). The
724 $\delta^{15}N$ value for atmospheric nitrogen being 0‰ (Sano and Pillinger, 1990; Nishizawa et al.,
725 2007), it cannot be clearly distinguished from the values measured in the N_2-H_2-CH_4 and N_2-
726 rich samples considering potential sampling bias plus analytical uncertainties of the
727 measurements. Although these results are compatible with an atmospheric nitrogen
728 component in the N_2-H_2-CH_4 and N_2-rich gas mixtures, this atmospheric component is not a
729 contamination as shown by the $N_2/^{36}Ar$ ratios for instance. This N_2 might thus be issued from
730 pore water trapped in the sediments (initial ASW) below the ophiolites or from the
731 metamorphism of clays from the sediments underthrusted below the ophiolitic units.
732 However, such a nitrogen isotopic value is not a clear diagnostic. Although it is compatible
733 with an atmospheric value, it does not exclude other origins like deeper components from
734 mantle and/or crust because a multiple origin of nitrogen is indeed supported by the results of
735 the noble gas analyses.
736 Noble gas contents suggest that there are at least two different sources of N_2. The plot of R/Ra
737 versus $^{20}Ne/^{4}He$ (Fig. 10) shows that the N_2-bearing gases are ranging on a mixing line
738 between the crust and the atmospheric end-member. In the H_2-rich type, the $N_2/^{36}Ar$ ratio is
739 close to the air and ASW ratios (Fig. 12A). This implies that N_2 in this gas originates from the
740 atmosphere and was carried by an aquifer equilibrated with the atmosphere or that the main
741 nitrogen component is acquired during the gas migration upwards through the aquifer. The
742 other samples (N_2-H_2-CH_4 and N_2-rich) do not align on these atmospheric ratios. They display
743 a nitrogen enrichment relative to ^{36}Ar (Fig. 12A) and the contents are much too high to be
744 only due to extraction from an aquifer related to free gas flows toward the surface.
745 From the plots of figures 12A and B, it can be inferred that N_2-rich type gases in Oman and
746 New Caledonia consist of a mixture of an atmospheric component and an almost pure
747 nitrogen end-member. The proportion of the nitrogen component varies in a large range (from
748 10 to 90% mol). ^{4}He is mainly a radiogenic product issued from the continental crust. It
749 cannot be produced in such amounts by mantle-derived ultrabasic rocks. Thus, the N_2-rich
750 gases can be interpreted as a crustal gas with a ^{4}He component. A potential interpretation for
751 the origin of deep N_2 could be that it was produced in the sediments and/or metasediments
752 buried under the ophiolitic units. In this case, the source could be the interstitial water in the

753 sediments and/or the solid matrix of the sediments (organic matter or ammonium in clay
754 sediments).
755
756 **Conclusion**
757
758 Integrating the results of previous studies and original results in different areas of the world,
759 this multi-tracer approach provided new insights on gas seepages in ophiolitic contexts. Four
760 types of gas mixtures were defined, three of them being associated with water springs and
761 characterized by the presence of N_2, CH_4 in proportions under 20 mol% and the presence of
762 H_2 within the ultra-basic springs. The fourth type corresponds to focused gas flows seeping
763 out directly from fractures (without water flow) and characterized by high proportions of CH_4
764 and low N_2. In all cases, H_2 is interpreted as a consequence of oxidation of Fe^{II}-rich minerals
765 present in the ophiolitic rocks (even though a contribution by microorganisms by dark
766 fermentation processes cannot be ruled out). Taking into account the pH conditions associated
767 with the H_2 generation, Fe^{III}-bearing mineral were formed at the vicinity of the sites of
768 oxidation of Fe^{II}-bearing mineral without an important mobility of Fe^{2+}. A relatively shallow
769 H_2 production is substantiated in the H_2-rich gas type by its association with quasi-
770 atmospheric noble gases. It is consistent with the D/H isotopic data of H_2 that may correspond
771 to a fluid rock reaction occurring at low temperature (probably below 50°C), whereas higher
772 temperatures are suspected for the H_2 production in the N_2-H_2-CH_4 gas type and notably in the
773 H_2-CH_4 gas type (probably above 100°C locally). The preservation of H_2 in the gas is directly
774 related to extreme limitation of carbon in the geological setting. It is probably related to the
775 carbon capture associated with massive precipitation of carbonates due to high-pH
776 conditions. Concerning CH_4, multiple origins are supported by the carbon isotopic data. The
777 carbon and hydrogen sources are various. Both, a primary CH_4 (from H_2O reacting with DIC)
778 and a secondary CH_4 (from an H_2 intermediate reacting with a C source) are suspected for the
779 H_2-CH_4 gas type and for N_2-H_2-CH_4 and H_2-rich gas types, respectively. In the gas mixtures,
780 N_2 appears to have two distinct origins: an atmospheric component and a deep crustal
781 component, as it was highlighted by the noble gas analyses. The different processes described
782 involve different types of fluids, which are: a shallow meteoric fluid, a crustal fluid carrying
783 metamorphic N_2, a deep mantle originating fluid carrying primordial CO_2. Depending on the
784 location with respect to the geodynamical context (Fig. 14), these different fluids interact and
785 mix in different proportions, yielding the types of gas mixture observed at the surface
786 seepages. The shallower kitchen is interpreted as the H_2-rich gas type from meteoric water

interacting with the ophiolite. The deepest kitchen is interpreted as the H_2-CH_4 gas type from a deep fluid (carrying CO_2 from the mantle, or from dissolved carbonates or organic carbon) interacting with the ophiolite. H_2-CH_4 gas flows are generally more localized (focused) and these flows are generally higher than the other H_2-bearing gas flows. This is probably due to the fact that they are generated at greater depth and at higher temperature conditions. This probably induces the individualization of a gas phase preventing H_2 to react during the rise toward the surface, notably by preventing any biological consumption of H_2 which required an aqueous media. The N_2-bearing fluids are probably generated mostly from the sediments located below the ophiolitic units and migrate upwards forming the N_2-rich gas type when reaching the surface or the N_2-H_2-CH_4 type if mixing occurs between the N_2-rich and the H_2-rich types (Fig. 14).

Acknowledgements

The authors would like to thank Georges Ceuleneer for his precious help and knowledge on the field in Oman, Mr Al Attaly for his enthusiasm towards our research and the information and help provided in Oman, Americus Perez and Zaymon Calucin for their help on the field in the Philippines, Christophe Chevillon and François Leborgne from the « Province Sud de Nouvelle-Calédonie, service de la mer et de la protection du lagon » who helped us very efficiently in New-Caledonia, Long Li for the nitrogen isotopes measurements performed at the IPGP. This work was achieved on IFPEN funds.

809

810 **References**

811

812 Abrajano, T. A., Sturchio, N. C., Bohlke, J. K., Lyon, G. L., Poreda, R., Stevens, C., 1988.
813 Methane-hydrogen gas seeps, Zambales Ophiolite, Philippines: Deep or shallow origin?
814 Chemical Geology, 71(1-3), 211–222. doi:10.1016/0009-2541(88)90116-7

815 Abrajano, T. A., Sturchio, N. C., Kennedy, B. M., Lyon, G. L., Muehlenbachs, K., Bohlke, J.
816 K., 1990. Geochemistry of reduced gas related to serpentinization of the Zambales
817 ophiolite, Philippines. Applied Geochemistry, 5(5-6), 625–630. doi:10.1016/0883-
818 2927(90)90060-I

819 Abrajano, J, Telling, J, Villiones, R, 2006. Methane-Hydrogen Generation in the Zambales
820 Ophiolite (Philippines) Revisited. AGU abstract.

821 Allen, D. E., Seyfried, W.E., 2004. Serpentinization and heat generation: constraints from
822 Lost City and Rainbow hydrothermal systems, Geochimica et Cosmochimica Acta 68, 6,
823 1347-1354.

824 Arai, S., Kadoshima, K., Morishita, T., 2006. Widespread arc-related melting in the mantle
825 section of the northern Oman ophiolite as inferred from detrital chromian spinels. Journal
826 of the Geological Society, 163, 869-879.

827 Balabane, M., Galimov, E., Hermann, M., Letolle, R., 1987. Hydrogen and carbon isotope
828 fractionation during experimental production of bacterial methane. Org. Geochem.11,
829 115–119.

830 Ballentine, C.J., Burnard, P. G., 2002. Production, release and transport of Noble Gases in the
831 continental crust. In “Noble Gases in Geochemistry and Cosmoschemistry”, Review in
832 Mineralogy and Geochemistry. 47, 481-538.

833 Ballentine, C. J., Sherwood Lollar, B., 2002a. Regional groundwater focusing of nitrogen and
834 noble gases into the Hugoton-Panhandle giant gas field, USA. Geochimica et
835 Cosmochimica Acta 66, 2483–2497.

836 Ballentine, C.J., Burgess, R., Marty, B. 2002b. Tracing fluid origin, transport and interaction
837 in the crust, D.R. Porcelli, C.J. Ballentine, R. Weiler (Eds.), Noble Gases in
838 Geochemistry and Cosmochemistry. Reviews in Mineralogy & Geochemistry, 47, 539–
839 614.

840 Barnes, I., Lamarche, V. C., Himmelberg, G., 1967. Geochemical evidence of present-day
841 serpentinization. Science (New York, N.Y.), 156 (3776), 830–832. doi:10.1126/science.
842 156.3776.830
843 Barnes, I., O'Neil, J. R., Trescases, J. J., 1978. Present day serpentinization in New
844 Caledonia, Oman and Yugoslavia. Geochimica et Cosmochimica Acta, 42(1), 144–145.
845 doi:10.1016/0016-7037(78)90225-9
846 Berndt, M.E., Allen, D.E., Seyfried, W.E. Jr, 1996. Reduction of CO2 during serpentinization
847 of olivine at 300°C and 500 bar. Geology 24, 351-354.
848 Boulart, C., Chavagnac, V., Minnin, C., Delacourt, A., Ceuleneer, G., Hoareau, G. 2013.
849 Difference in gas ventingfrom ultramafic-hosted warm springs: the axample of Oman and
850 Voltri ophiolites. Ofioliti 38(2), 143-156.
851 Bottinga, Y., 1969. Calculated fractionation factors for carbon and hydrogen isotope exchange
852 in the system calcite-carbon dioxide-graphite-methane-hydrogen-water vapor. Geochim.
853 Cosmochim. Acta 33, 49–64.
854 Boulart, C., Chavagnac, V., Monnin, C., Delacour, A., Ceuleneer, G., Hoareau, G. 2013.
855 Differences in gas venting from ultramafic-hosted warm springs: the example of Oman
856 and Voltri Ophiolites. Ofioliti 38, 2 , 143-156.
857 Bozcu, A., Yagmurlu, F., 2001. Correlation of sedimentary units in the Weseter Taurides
858 from the point of petroleum geology. 4th International Symposium on Eastern
859 Mediterranean Geology, Isparta, Turkey, 139-148.
860 Bradley, A.S., Summons, R.E., 2010. Multiple origins of methane at the Lost City
861 hydrothermal field. Earth and Planetary Science Letters 294, 34-41.
862 Brazelton, W.J., Schrenk, M.O., Kelley, D.S., Baross, J.A., 2006. Methane- and Sulfur-
863 Metabolizing Microbial Communities Dominate the Lost City Hydrothermal Field
864 Ecosystem. Environ. Microbiol. vol. 72 no. 96257-6270. doi: 10.1128/AEM.00574-
865 06Appl.
866 Brazelton, W.J., Morrill, P.L., Szponar, N., Schrenk, M.O., 2013. Bacterial Communities
867 Associated with Subsurface Geochemical Processes in Continental Serpentinite Springs.
868 Appl. Environ. Microbiol., 79(13):3906. DOI: 10.1128/AEM.00330-13.
869 Bruni, J., Canepa, M., Chiodini, G., Cioni, R., 2002. Irreversible water-rock mass transfer
870 accompanying the generation of the neutral, Mg-HCO3 and high-pH, Ca-OH spring
871 waters of the Genova province, Italy. Applied Geochemistry, 17, 455–474.

Burnard, P., Zimmermann, L., Sano, Y., 2013. The Noble Gases as Geochemical Tracers: History and Background. In The Noble Gases as Geochemical Tracers, Editor : Pete Burnard, Springer, 1-15.

Buzek, F., Onderka, V., VanCurat, P., Wolf, I., 1994. Carbon isotope study of methane production in a town gas storage reservoir. Fuel 73, 5, 747-752.

Cardace, D., Meyer-Dombard, D.R., Woycheese, K.M., Arcilla C.A., 2015. Feasible Metabolisms in High pH Springs of the Philippines. Front Microbiol. 6, 10. Published online 2015 Feb 10. doi: 10.3389/fmicb.2015.00010.

Ceuleneer, G., 1991. Evidence for a paleo-spreading center in the Oman ophiolite: mantle structures in the Maqsad area. 5, 147-173.

Charlou, J.L., Donval, J.P., Fouquet, Y., Jean-Baptiste, P., Holm, N., 2002. Geochemistry of high H_2 and CH_4 vent fluids issuing from ultramafic rocks at the Rainbow hydrothermal field (36°14'N, MAR). Chemical Geology 191, 345–359.

Chavagnac, V., Monnin, C., Ceuleneer, G., Boulart, C., Hoareau, G., 2013. Characterization of hyperalkaline fluids produced by low-temperature serpentinization of mantle peridotites in the Oman and Ligurian ophiolites. Geochemistry Geophysics Geosystems G3, 14(7), 2496-2522. DOI: 10.1002/ggge.20147.

Cipolli, F., Gambardella, B., Marini, L., Ottonello, G., Vetuschi Zuccolini, M., 2004. Geochemistry of high-pH waters from serpentinites of the Gruppo di Voltri (Genova, Italy) and reaction path modeling of CO_2 sequestration in serpentinite aquifers. Applied Geochemistry, 19(5), 787–802. doi:10.1016/j.apgeochem.2003.10.007

Coveney, R. M. J., Goebel, E. D., Zeller, E. J., Dreschhoff, G.A. M., & Angino, E. E., 1987. Serpentinization and origin of hydrogen gas in Kansas. AAPG Bulletin, 71, 39–48.

De Boer, J. Z., Chanton, J., Zeitlhöfler, M., 2007. Homer's chimaera fires (SW of Antalya/Turkey); burning abiogenic methane gases; are they generated by a serpentinization process related to alkalic magmatism? Zeitschrift Der Deutschen Gesellschaft Für Geowissenschaften, 158(4), 997–1003. doi:10.1127/1860-1804/2007/0158-0997

Deville, E., Prinzhofer, A., Pillot, D., Vacquand, C., Sissman, O., 2010. Peridote-water interaction generating migration pathways of N_2-H_2-CH_4-rich fluids in subduction context: Common processes in the ophiolites of Oman, New-Caledonia, Philippines and Turkey. American Geophysical Union Transactions, T13A-2184D.

Deville, E., Prinzhofer, A., Pillot, D., Vacquand, C., 2011. Natural flows of H_2 and associated diagenetic processes of atmospheric CO_2 capture and sequestration: a study

in the ophiolites of Oman. Proceedings of the Offshore Mediterranean Conference, OMC 2011, Paper# ISBN 9788894043686, 9 pages.

Deville, E., Prinzhofer, A., 2016. The origin of N_2-H_2-CH_4-rich natural gas seepages in ophiolitic context: A major and noble gases study of fluid seepages in New Caledonia. Chemical Geology, 440, 139–147.

Encarnacion, J., Mukasa, S. B., Evans, C. A., 1999. Subduction components and the generation of arc-like melts in the Zambales ophiolite, Philippines: Pb, Sr and Nd isotopic constraints. Chemical Geology 156, 343-357.

Etiope, G., Schoell, M., Hosgörmez, H., 2011. Abiotic methane flux from the Chimaera seep and Tekirova ophiolites (Turkey): Understanding gas exhalation from low temperature serpentinization and implications for Mars. Earth and Planetary Science Letters 310 (1-2), 96–104. doi:10.1016/j.epsl.2011.08.001

Etiope, G., Sherwood-Lollar, B., 2013. Abiotic methane on Earth. Rev. Geophys. 51, 276-299, doi.org/10. 002/rog.20011.,

Etiope, G., Vance, S., Christensen, L.E., Marques, J.M., Ribeiro da Costa, I., 2013. Methane in serpentinized ultramafic rocks in mainland Portugal. Mar. Petroleum Geol. 45, 12–16.

Etiope, G,, Ionescu, A., 2015. Low-temperature catalytic CO2 hydrogenation with geological quantities of ruthenium: a possible abiotic CH4 source in chromitite-rich serpentinized rocks. Geofluids 15, 438–45

Etiope, G, 2017. Methane origin in the Samail ophiolite: Comment on “Modern water/rock reactions in Oman hyperalkaline peridotite aquifers and implications for microbial habitability” Geochim. Cosmochim. Acta 179, 217–241.

Evans, B.W., 2008. Control of the products of serpentinization by the Fe2+Mg_1 exchange potential of olivine and orthopyroxene, J. Petrol., 49, 1873–1887, doi:10.1093/petrology/egn050.

Foustoukos, D.I., Seyfried, W.E. Jr., 2004. Hydrocarbons in hydrothermal fluids: the role of chromium-bearing catalysts. Science 304, 1002-1005.

Fu, Q., Foustoukos, D.I., Seyfried, W.E., 2008. Mineral catalyzed organic synthesis in hydrothermal systems: an experimental study using time-of-flight secondary ion mass spectrometry. Geophys. Res. Lett. 35 (ISI:000255201300005).

Gallant, R. M., Von Damm, K. L., 2006. Geochemical controls on hydrothermal fluids from the Kairei and Edmond Vent Fields, 23°–25°S, Central Indian Ridge. G3 Geochemistry, Geophysics, Geosystems, 7, 6, doi:10.1029/2005GC001067.

939 Garcia, B., Beaumont, V., Perfetti, E., Rouchon, V., Blanchet, D., Oger, P., Dromart, G., Huc,
940 A.-Y., Haeseler, F., 2010. Experiments and geochemical modelling of CO_2 sequestration
941 by olivine: Potential, quantification. Applied Geochemistry 25, 1383–1396.
942 Glover, C. P., Robertson, A. H. F., 1998a. Role of regional extension and uplift in the Plio-
943 Pleistocene evolution of the Aksu Basin, SW Turkey. Journal of the Geological Society,
944 155, 365-387.
945 Glover, C., Robertson, A., 1998b. Neotectonic intersection of the Aegean and Cyprus tectonic
946 arcs: extensional and strike-slip faulting in the Isparta Angle, SW Turkey.
947 Tectonophysics 298, 103-132.
948 Guélard J., Beaumont V., Guyot F., Pillot D., Jezequel D., Ader M., Newell K. D., Deville E.
949 2017. Natural H_2 in Kansas: deep or shallow origin? G^3 Geochemistry, Geophysics and
950 Geosystems, 18, DOI: 10.1002/2016GC006544.
951 Hawkins, D. E., Evans, C. A., 1983. Geology of the Zambales Range, Luzon, Philippines:
952 Ophiolite derived from an island arc-back arc pair. AGU Geophys. Mono., 95-123.
953 Hopson, C. A., Coleman, R. G., Gregory, R. T., Pallister, J. S., Bailey, E. H., 1981. Geologic
954 Section Through the Samail Ophiolite and Associated Rocks Along A Muscat-Ibra
955 Transect, Southeastern Oman Mountains. Journal of Geophysical Research 86, 2527-
956 2544.
957 Horibe Y., Craig H., 1995. D/H fractionation in the system methane-hydrogen-water.
958 Geochim. Cosmochim. Acta 59, 5209–5217.
959 Horita, J., Berndt, M.E., 1999. Abiogenic methane formation and isotopic fractionation under
960 hydrothermal conditions. Science 285, 1055-1057.
961 Hosgörmez, H., 2007. Origin of the natural gas seep of Cirali (Chimera), Turkey: Site of the
962 first Olympic fire. Journal of Asian Earth Sciences 30 (1), 131–141.
963 Hosgörmez, H., Etiope, G., Yalçin, M. N., 2008. New evidence for a mixed inorganic and
964 organic origin of the Olympic Chimaera fire (Turkey): a large onshore seepage of
965 abiogenic gas. Geofluids 8 (4), 263–273. doi:10.1111/j.1468-8123.2008.00226.x
966 Ikorsky, S.V., Gigashvili, G.M., Lanyov, V.S., Narkotiev, V.D., Petersilye, I.A., 1999. The
967 investigation of gases during the Kola superdeep borehole drilling (to 11.6 km). Geol. Jb.
968 D107, 145-152.
969 Jenden, P.D., Kaplan, I.R., Poreda, R.J., Craig H., 1988. Origin of nitrogen-rich natural gases
970 in the California Great Valley: Evidence from helium, carbon and nitrogen isotope ratios.
971 Geochim. Cosmochim. Acta 52, 851-861.

Juteau, T., Nicolas, A., Dubessy, J., Fruchard, J. C., Bouchez, J. L., 1977. Structural Relationships in Antalya Ophiolite Complex, Turkey - Possible Model for An Oceanic Ridge. Geological Society of America Bulletin 88, 1740-1748.

Kawagucci et al., 2016. Fluid chemistry in the solitaire and Dodo hydrothermal fields of the Centram Indian Ridge. Geofluids 16, 988-1005.

Kelemen, P.B., Matter, J., Streit, E.E., Rudge, J.F., Curry W.B., Blusztajn, J., 2011. Rates and Mechanisms of Mineral Carbonation in Peridotite: Natural Processes and Recipes for Enhanced, in situ CO_2 Capture and Storage. Annual Review of Earth and Planetary Sciences, 39, 545-576.

Kelley, D.S., Früh-Green, G.L. 1999. Abiogenic methane in deep-seated mid-ocean ridge environments: Insights from stable isotope analyses. Journal of Geophysical Research 104 (B5), 10439-10460. doi: 10.1029/1999JB900058.

Kelley, D.S., Karson, J.A., Früh-Green, G.L., Butterfield, D.A., Lilley, M.D., Olson, E., Schrenk, M.O., Roe, K.K., Lebon, G.T., Rivizzigno, P., AT3–60 Shipboard Party, 2001. An off-axis hydrothermal field near the Mid-Atlantic Ridge at 30°N. Nature 412, 145–149.

Kelley, D.S., Karson, J.A., Fruh, G.L., Yoerger, D.R., Shank, T.M., Butterfield, D.A., Hayes, J.M., Schrenk, M.O., Olson, E.J., Proskurowski, G., Jakuba, M., Bradley, A., Larson, B., Ludwig, K., Glickson, D., Buckman, K., Bradley, A.S., Brazelton, W.J., Roe, K., Bernasconi, S.M., Elend, M.J., Lilley, M.D., Baross, J.A., Summons, R.E., Sylva, S.P., 2005. A serpentinite-hosted ecosystem: the Lost City hydrothermal field. Science 307, 1428–1434.

Klein, F., Bach, W., Jöns, N., McCollom, T., Moskowitz, B., Berquó, T., 2009. Iron partitioning and hydrogen generation during serpentinization of abyssal peridotites from 15°N on the Mid-Atlantic Ridge. Geochimica et Cosmochimica Acta 73,22, 6868–6893. doi:10.1016/j.gca.2009.08.021

Klein, F., Grozeva, N.G., Seewald, J.S., McCollom, T.M., Humphris, S.E., Moskowitz, B., Berquó, T.S., Kahl, W.-A., 2015. Experimental constraints on fluid-rock reactions during incipient serpentinization of harzburgite. American Mineralogist 100, 991–1002.

Kumagai, H., Nakamura, K., Toki, T., Morishita, T., Okino, K., Ishibashi, J.-I., Tsunogai, U., Kawagucci, S., Gamo, T., Shibuya, T., Sawaguchi, T., Neo, N., Joshima, M., Sato, T., Takai, K., 2008. Geological background of the Kairei and Edmond hydrothermal fields along the Central Indian Ridge: Implications of their vent fluids' distinct chemistry. Geofluids 8, 239–251.

1006 Larin, N., Zgonnik, V., Rodina, S., Deville, É., Prinzhofer, A., Larin, V.N., 2015. Natural
1007 molecular hydrogen seepages associated with surficial, rounded depression on the
1008 European craton in Russia. Natural Resources Research, 24, 3, 363-383. DOI:
1009 10.1007/s11053-014-9257-5.
1010 Launay, J., Fontes, J.C. 1985. Les sources thermales de Prony (Nouvelle-Calédonie) et leurs
1011 précipités chimiques. Exemple de formation de brucite primaire. Géologie de la France,
1012 1, 83-100.
1013 Marcaillou, C., Muñoz, M., Vidal, O., Parra, T., Harfouche, M., 2011. Mineralogical evidence
1014 for H_2 degassing during serpentinization at 300°C/300bar. Earth and Planetary Science
1015 Letters 303 (3-4), 281–290. doi:10.1016/j.epsl.2011.01.006
1016 Mayhew, L. E., Ellison, E. T., McCollom, T. M., Trainor, T. P., Templeton, a. S., 2013.
1017 Hydrogen generation from low-temperature water–rock reactions. Nature Geoscience 6
1018 (6), 478–484. doi:10.1038/ngeo1825
1019 McCollom, T. M., Bach, W., 2009. Thermodynamic constraints on hydrogen generation
1020 during serpentinization of ultramafic rocks. Geochimica et Cosmochimica Acta 73 (3),
1021 856–875. doi:10.1016/j.gca.2008.10.032
1022 McCollom, T.M., Seewald, J.S., 2001. A reassessment of the potential for reduction of
1023 dissolved CO2 to hydrocarbons during serpentinization of olivine. Geochimica et
1024 Cosmochimica Acta 65, 3769-3778.
1025 McCollom, T.M., Lollar, B.S., Lacrampe-Couloume, G., Seewald, J.S., 2010. The influence
1026 of carbon source on abiotic organic synthesis and carbon isotope fractionation under
1027 hydrothermal conditions. Geochim. Cosmochim. Acta 74, 2717–2740.
1028 McCollom, TM., 2016. Abiotic methane formation during experimental serpentinization of
1029 olivine. Proc Natl Acad Sci U S A. 113(49):13965-13970.
1030 Meyer-Dombard, D.R., Woycheese, K.M., Yargıçoğlu, E.N., Cardace, D., Güleçal, Y., Temel,
1031 M., Shock, E., 2015. High pH microbial ecosystems in a newly discovered, ephemeral,
1032 serpentinizing fluid seep at Yanartaş (Chimaera), Turkey. Front Microbiol. 5, 723, doi:
1033 10.3389/fmicb.2014.00723.
1034 Milesi, V., Prinzhofer, A., Guyot, F., Benedetti, M., Rodrigues, R., 2016. Contribution of
1035 siderite–water interaction for the unconventional generation of hydrocarbon gases in the
1036 Solimões basin, north-west Brazil. Marine and Petroleum Geology 71, 168-182.
1037 Miller, H.M., Matter, J.M., Kelemen, P., Ellison, E.T., Conrad, M.E., Fierer, N., Ruchala, T.,
1038 Tominaga, M., Templeton, A.S., 2016. Modern water/rock reactions in Oman

hyperalkaline peridotite aquifers and implications for microbial habitability. Geochimica et Cosmochimica Acta 179, 217-241.

Miller, H.M., Matter, J.M., Kelemen, P., Ellison, E.T., Conrad, M.E., Fierer, N., Ruchala, T., Tominaga, M., Templeton, A.S., 2017. Reply to ‘‘Methane origin in the Samail ophiolite: Comment on ‘Modern water/rock reactions in Oman hyperalkaline peridotite aquifers and implications for microbial habitability’. Geochimica et Cosmochimica Acta 197, 471–473.

Monnin, C., Chavagnac, V., Boulart, C., Ménez, B., Gérard, M., Gérard, E., Quéméneur, M., Erauso, G., Postec, A., Guentas-Dombrowski, L., Payri, C., Pelletier, B., 2014. The low temperature hyperalkaline hydrothermal system of the Prony Bay (New Caledonia). Biogeosciences Discuss. 11, 6221–6267.

Moody, J.B., 1976. Serpentinization: a review. Lithos 9, 125–138.

Morrill, P.L., Kuenen, J.G., Johnson, O.J., Suzuki, S., Rietze, A., Sessions, A.L., Fogel, M.L., Nealson, K.H., 2013. Geochemistry and geobiology of a present-day serpentinization site in California: The Cedars. Geochimica et Cosmochimica Acta 109, 222–240.

Neal, C., Stanger, G., 1983. Hydrogen generation from mantle source rocks in Oman. Earth and Planetary Science Letters 66, 315–320. doi:10.1016/0012-821X(83)90144-9

Neal, C., Stanger, G., 1984. Calcium and magnesium hydroxide precipitation from alkaline groundwaters in Oman, and their significance to the process of serpentinization. Mineral. Mag. 48, 237–241.

Neal, C., Stanger, G., 1985. Past and present serpentinisation of ultramafic rocks; an example from the Semail ophiolite nappe of Northern Oman. In J. I. Dever (Ed.), The Chemistry of Weathering, D. Reidel Publishing Company, 249–275.

Neubeck, A., Duc, N. T., Bastviken, D., Crill, P., Holm, N. G., 2011. Formation of H_2 and CH_4 by weathering of olivine at temperatures between 30 and 70°C. Geochemical Transactions 12 (1), 6. doi:10.1186/1467-4866-12-6

Neubeck A., Nguyen D.T., Etiope G., 2016. Low-temperature dunite hydration: evaluating CH_4 and H_2 production from H_2O and CO_2 Geofluids 16, 408–42.

Nicolas, A., Boudier, F., Ildefonse, B., 1996. Variable crustal thickness in the Oman ophiolite: Implication for oceanic crust. Journal of Geophysical Research-Solid Earth 101, 17941-17950.

Nicolas A., Boudier F., Ildefonse B., Ball E., 2000. Accretion of Oman and United Arab Emirates ophiolite – Discussion of a new structural map. Marine Geophysical Researches 21, 147–179.

Nicolas, A., Violette, J. F., 1982. Mantle Flow at Oceanic Spreading Centers - Models Derived from Ophiolites. Tectonophysics 81, 319-339.

Nishizawa, M., Sano, Y., Ueno, Y., Maruyama, S. 2007. Speciation and isotope ratios of nitrogen in fluid inclusions from seafloor hydrothermal deposits at ~ 3.5 Ga. Earth and Planetary Science Letters 254,3-4, 332-344; DOI: 10.1016/j.epsl.2006.11.044.

Okland, I, Huang, S., Thorseth, I.H., Pedersen, R.B., 2014. Formation of H_2, CH_4 and N-species during low-temperature experimental alteration of ultramafic rocks. Chemical Geology 387, 22–34.

Okumura, T., Kawagucci, S., Saito, Y., Matsui, Y., Takai, K., Imachi, H., 2016. Hydrogen and carbon isotope systematics in hydrogenotrophic methanogenesis under H2-limited and H2-enriched conditions: implications for the origin of methane and its isotopic diagnosis. Progress in Earth and Planetary Science) 3:14, DOI 10.1186/s40645-016-0088-3.

Oze, C., Sharma, M., 2005. Have olivine, will gas: Serpentinization and the abiogenic production of methane on Mars. Geophysical Research Letters, 32, L10203, doi:10.1029/2005GL022691,

Paris, J.P., 1981. Géologie de la Nouvelle-Calédonie. Mém. BRGM 133, 1–278.

Paukert, A. N., Matter, J. M., Kelemen, P. B., Shock, E. L., Havig, J. R., 2012. Reaction path modeling of enhanced in situ CO_2 mineralization for carbon sequestration in the peridotite of the Samail Ophiolite, Sultanate of Oman. Chemical Geology 330-331, 86–100. doi:10.1016/j.chemgeo.2012.08.013

Prinzhofer, A., 2013. Noble gases in oil and gas accumulations. In The Noble Gases as Geochemical Tracers, Editor : Pete Burnard, Springer, 225-247.

Prinzhofer, A., Deville, E., 2013. Origins of hydrocarbon gas seeping out from offshore mud volcanoes in the Nile delta. Tectonophysics 591, 52–61.

Proskurowski, G., Lilley, M. D., Kelley, D. S., Olson, E. J., 2006. Low temperature volatile production at the Lost City Hydrothermal Field, evidence from a hydrogen stable isotope geothermometer. Chemical Geology 229 (4), 331–343. doi:10.1016/j.chemgeo.2005.11.005

Proskurowski, G., Lilley, M.D., Seewald, J.S., Früh-Green, G.L., Olson, E.O., Lupton, J.E., Sylva, S.P., Kelley, D.S., 2008. Abiogenic hydrocarbon production at lost city hydrothermal field. Science 319, 5863, 604–607.

Python, M., Ceuleneer, G., 2003. Nature and distribution of dykes and related melt migration structures in the mantle section of the Oman ophiolite. Geochemistry Geophysics Geosystems, 4, 7, 8612, doi:10.1029/2002GC00035.

Robertson, A. H. F., Woodcock, N. H., 1980. Strike slip related sedimentation in the Antalya Complex, SW Turkey. Special publication of the International Association of Sedimentologists, 4, 127-145.

Sano, Y., Pillinger, C.T., 1990. Nitrogen isotopes and N2/Ar ratios in cherts: an attempt to measure time evolution of atmospheric δ15N value. Geochemistry Journal 24, 315–324.

Sano, Y., Urabe, A., Wakita, H., Wushiki, H., 1993. Origin of hydrogen-nitrogen gas seeps, Oman. Applied Geochemistry 8 (1), 1–8. doi:10.1016/0883-2927(93)90053-J

Seewald, J.S., Zolotov, M.Y., McCollom, T., 2006. Experimental investigation of single carbon compounds under hydrothermal conditions. Geochim. Cosmochim. Acta 70, 446–460.

Sherwood-Lollar, B., Fritz, P., Frape, S.K., Macko, S.A., Weise, S.M., Welhan, J.A., 1988. Methane occurrences in the Canadian shield. Chem. Geol. 71, 223–236.

Sherwood-Lollar, B., Frape, S.K., Fritz, P., Macko, S.A., Welhan, J.A., Blomqvist, R., Lahermo, P.W., 1993a. Evidence for bacterially generated hydrocarbon gas in Canadian Shield and Fennoscandian Shield rocks. Geochim. Cosmochim. Acta 57, 5073–5085.

Sherwood-Lollar, B., Frape, S.K., Weise, S.M., Fritz, P., Macko, S.A., Welhan, J.A., 1993b. Abiogenic methanogenesis in crystalline rocks. Geochim. Cosmochim. Acta 57, 5087–5097.

Sherwood-Lollar, B., Lacrampe-Couloume, G., Slater, G.F., Ward, J., Moser, D.P., Gihring, T.M., Lin, L.-H., Onstott, T.C., 2006. Unravelling abiogenic and biogenic sources of methane in the Earth's deep subsurface. Chemical Geology 226, 328– 339.

Sherwood-Lollar, B., Voglesonger, K., Lin, L.-H., Lacrampe-Couloume, G., Telling, J., Abrajano, T.A., Onstott, T.C., Pratt, L.M., 2007. Hydrogeologic controls on episodic H_2 release from Precambrian fractured rocks–Energy for deep subsurface life on Earth and Mars. Astrobiology 7, 971–986.

Shibuya, T., Yoshizaki, M., Sato, M., Shimizu, K., Nakamura, K., Omori, S., Suzuki, K., Takai, K., Tsunakawa H., Maruyama S., 2015. Hydrogen-rich hydrothermal environments in the Hadean ocean inferred from serpentinization of komatiites at 300 °C and 500 bar. Progress in Earth and Planetary Science 2, 46.

Suda, K., Ueno, Y.,Yoshizaki, M., Nakamura, H., Kurokawa K., Nishiyama, E., Yoshino, K., Hongoh, Y., Kawachi, K., Omori, S., Yamada, K., Yoshida, N., Maruyama, S., 2014.

Origin of methane in serpentinite-hosted hydrothermal systems: The CH_4–H_2–H_2O hydrogen isotope systematics of the Hakuba Happo hots spring. Earth and Planetary Science Letters 386, 112–125.

Szatmari, P., 1989. Petroleum formation by Fischer–Tropsch synthesis in plate tectonics. American Association of Petroleum Geologists Bulletin 73, 989–998.

Szponar, N, Brazelton, W.J., Schrenk, M.O., Bower, D.M., Steele, A., Morrill, P.L. 2013. Geochemistry of a continental site of serpentinization, the Tablelands Ophiolite, Gros Morne National Park: a Mars analogue. Icarus 224, 286–296, doi:10.1016/j.icarus.2012.07. 004.

Takai, K. , T. Gamo, U. Tsunogai, N. Nakayama, H. Hirayama, K. H. Nealson, and K. Horikoshi, 2004. Geochemical and microbiological evidence for a hydrogen-based, hyperthermophilic subsurface lithoautotrophic microbial ecosystem (HyperSLiME) beneath an active deep-sea hydrothermal field. Extremophiles 8, 269–282.

Takai K., K. Nakamura, T. Toki, U. Tsunogai, M. Miyazaki, J. Miyazaki, H. Hirayama, S. Nakagawa, T. Nunoura, K. Horikoshi., 2008. Cell proliferation at 122°C and isotopically heavy CH_4 production by a hyperthermophilic methanogen under high-pressure cultivation. Proceedings of the National Academy of Sciences 105, 31, 10949-10954.

Taran, Y.A., Kliger, G.A., Sevastianov, V.S., 2007. Carbon isotope effects in the open-system Fischer–Tropsch synthesis. Geochimica et Cosmochimica Acta 71, 4474–4487.

Vacquand C., 2011. Genèse et mobilité de l'hydrogène naturel: source d'énergie ou vecteur d'énergie stockable ? Ph.D thesis IFPEN-IPGP, 174 pages.

Valentine, D.L., Chidthaisong, A., Rice, A., Reeburgh, W.S., Tyler, S.C., 2004. Carbon and hydrogen isotope fractionation by moderately thermophilic methanogens. Geochim. Cosmochim. Acta 68, 1571–1590.

Welhan, J. A., Craig, H., 1979. Methane and hydrogen in East Pacific Rise hydrothermal fluids, Geophys. Res. Lett. 6, 829–831.

Woycheese, K.M., Meyer-Dombard, D.R., Cardace, D., Argayosa, A.M., Arcilla, C.A., 2015. Out of the dark: Transitional subsurface-to-surface microbial diversity in a terrestrial serpentinizing seep (Manleluag, Pangasinan, the Philippines). Frontiers in Microbiology, Special Issue: Portals to the Deep Biosphere. Front Microbiol. 6, 44, doi: 10.3389/fmicb.2015.00044 L82.

Yoshizaki, M., Shibuya, T., Suzuki, K., Shimizu, K., Nakamura, K., Takai, K., Omori, S., Maruyama, S., 2009. H_2 generation by experimental hydrothermal alteration of komatiitic

glass at 300°C and 500 bars: A preliminary result from on-going experiment. Geochemical Journal 43, e17 to e22.

Yumul, G. P., Dimalanta, C. B., Faustino, D. V., de Jesus, J. V., 1998. Translation and docking of an arc terrane: geological and geochemical evidence from the southern Zambales Ophiolite Complex, Philippines. Tectonophysics 293, 255-272.

Zgonnik, V., Beaumont, V., Deville, E., Larin, N., Pillot, D., Farrell, K., 2015. Evidences for natural hydrogen seepages associated with rounded subsident structures: the Carolina bays (Northern Carolina, USA), Progress in Earth and Planetary Science 2:31, DOI 10.1186/s40645-015-0062-5.

Zhou, Z., Ballentine, C.J., Kipfer, R., Schoell, M., Thibodeaux, S., 2005. Noble gas tracing of groundwater/coalbed methane interaction in the San Juan Basin, USA. Geochimica et Cosmochimica Acta 69, 5413-5428.

Zhu, Y., 2000. The isotopic compositions of molecular nitrogen : implications on their origins in natural gas accumulations. Chemical Geology 164, 3–4, 321–330.

1187

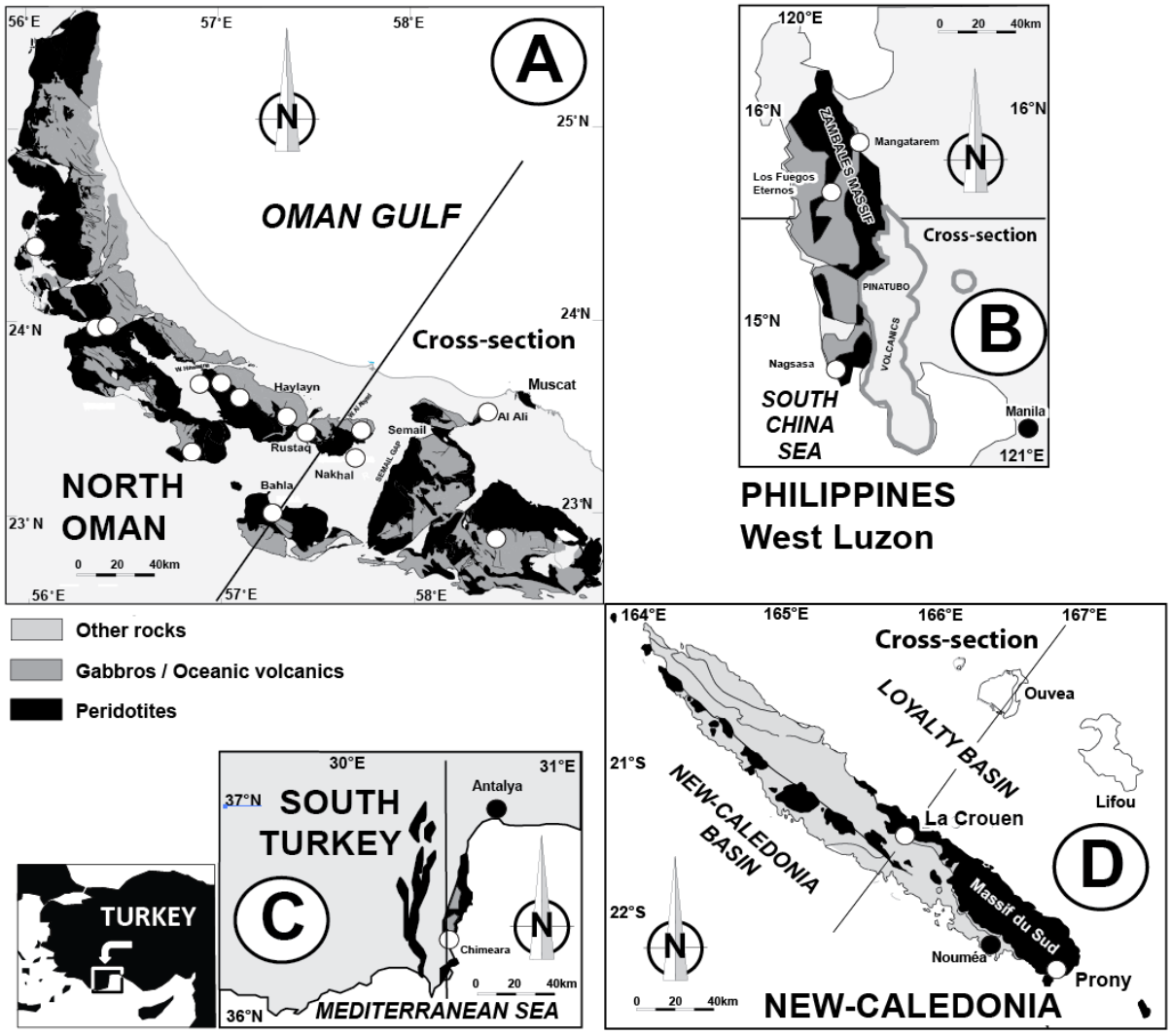

1188

1189 **Figure 1 –** Structural sketch-maps of the different sites studied in this work in Oman (A), the
1190 Philippines (B), Turkey (C) and New-Caledonia (D) (same scale), with the location of the
1191 sampling sites and the location of the cross-sections shown in figure 2. The gas seepages are
1192 associated with ophiolitic ultrabasic rocks. Gas was sampled from different types of seepages:
1193 gas seeping in water which originates from ultrabasic or hot springs and gas seeping from
1194 fractures without water flow.

1195

1196

1197

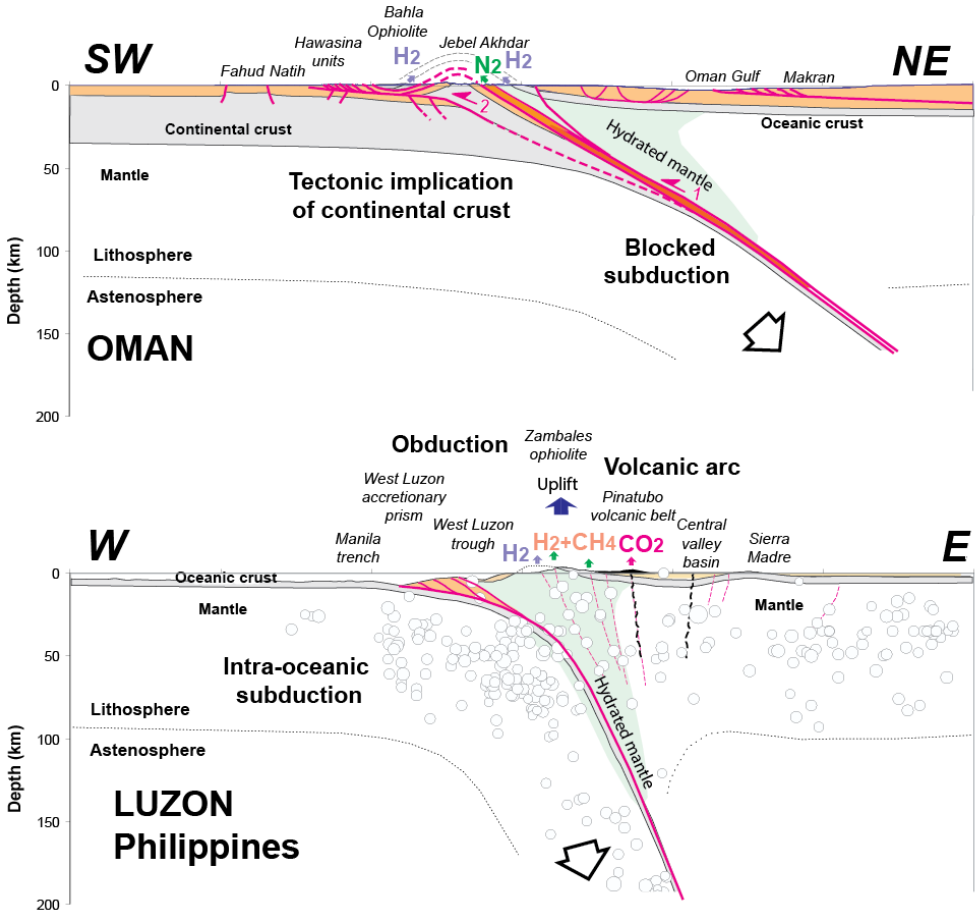
SW
NE
Bahla Ophiolite
Hawasina units
Jebel Akhdar
Fahud Natih
Oman Gulf
Makran
H2
N2
H2
Continental crust
Oceanic crust
Hydrated mantle
Mantle
Tectonic implication of continental crust
Blocked subduction
Lithosphere
Astenosphere
OMAN
Depth (km)
0
50
100
150
200
Obduction
Zambales ophiolite
Volcanic arc
West Luzon accretionary prism
Uplift
Pinatubo volcanic belt
Manila trench
West Luzon trough
H2
H2+CH4
CO2
Central valley basin
Sierra Madre
W
E
Oceanic crust
Mantle
Mantle
Intra-oceanic subduction
Hydrated mantle
Lithosphere
Astenosphere
LUZON
Philippines

1198

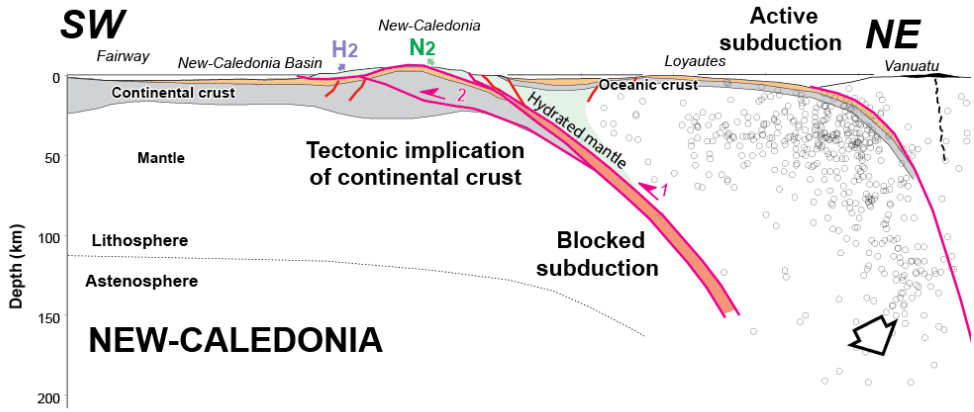
SW
NE
Fairway
New-Caledonia Basin
New-Caledonia
H2
N2
Active subduction
Loyautes
Vanuatu
Continental crust
Oceanic crust
Hydrated mantle
Mantle
Tectonic implication of continental crust
Blocked subduction
Lithosphere
Astenosphere
NEW-CALEDONIA
Depth (km)
0
50
100
150
200

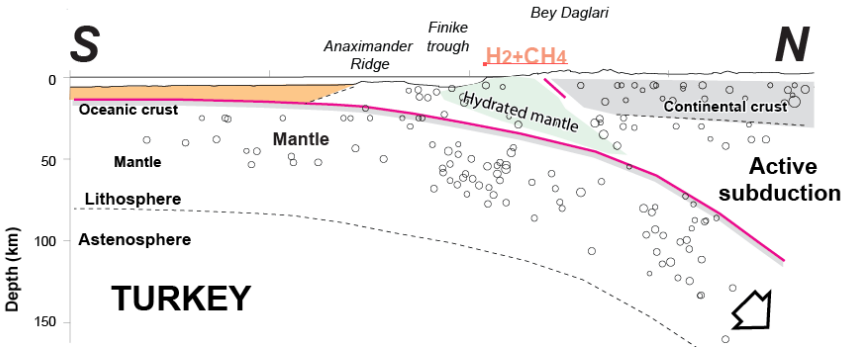
S
N
Bey Daglari
Finike trough
Anaximander Ridge
H2+CH4
Oceanic crust
Hydrated mantle
Continental crust
Mantle
Mantle
Active subduction
Lithosphere
Astenosphere
TURKEY
Depth (km)
0
50
100
150

1199

1200 **Figure 2 -** Geological cross-sections of the different sites studied in this work (same scale;
1201 earthquake epicenters from USGS data base). A 2D cross-section for the area of Chimaera in
1202 Turkey is not shown because of too complex 3D geometry in a transform fault system.

1203

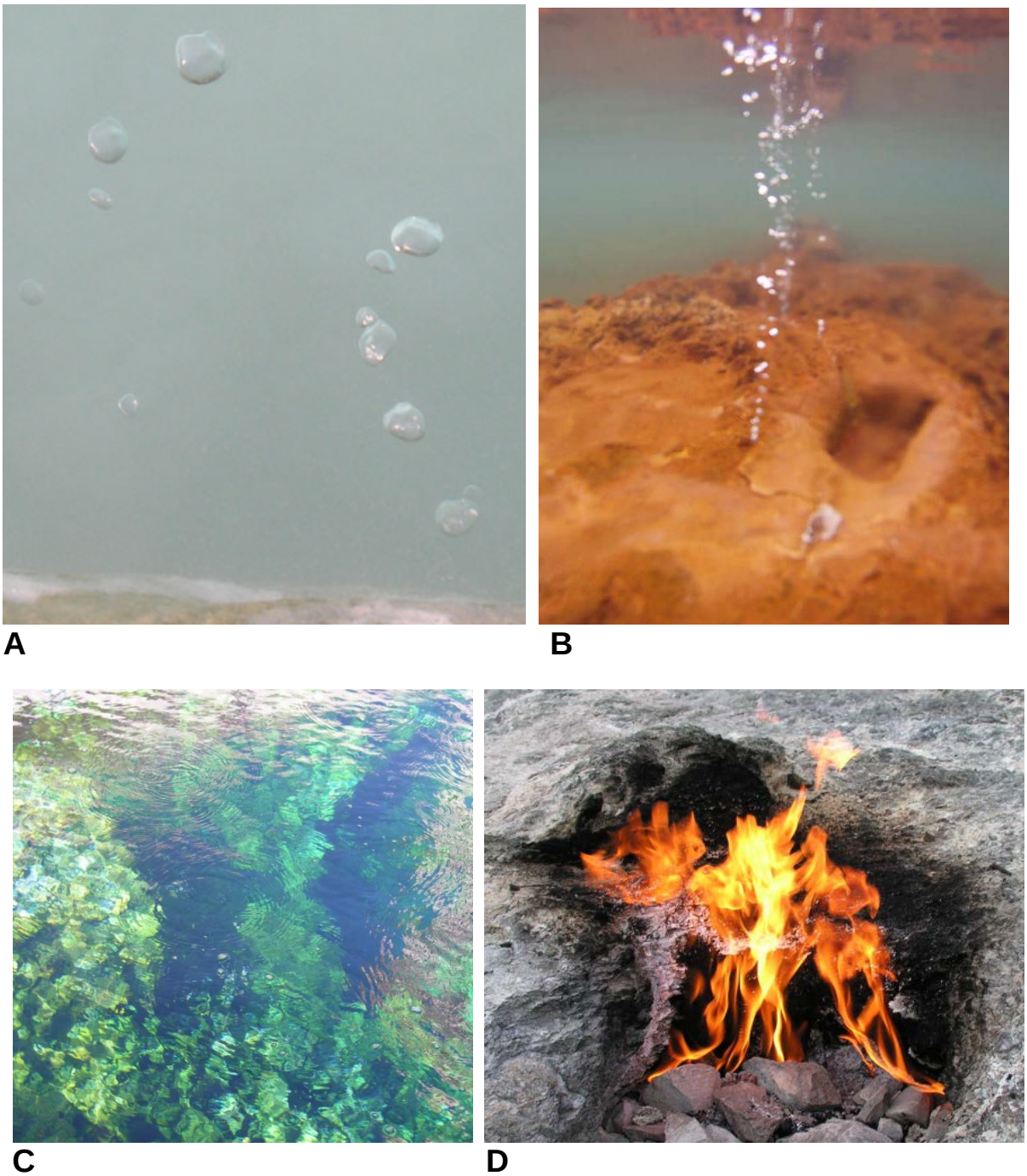

Figure 3 – Examples of gas seepages. **A:** Bubbling H_2-rich gas flow in ultra-basic water (Oman). **B:** Bubbling N_2-H_2-CH_4 gas flow (foreshore of the Baie du Carénage, New Caledonia). **C:** Bubbling N_2–rich gas flow (Rustaq, Oman). **D**: Burning H_2 -CH_4 gas flow (Chimaera, Turkey).

1215

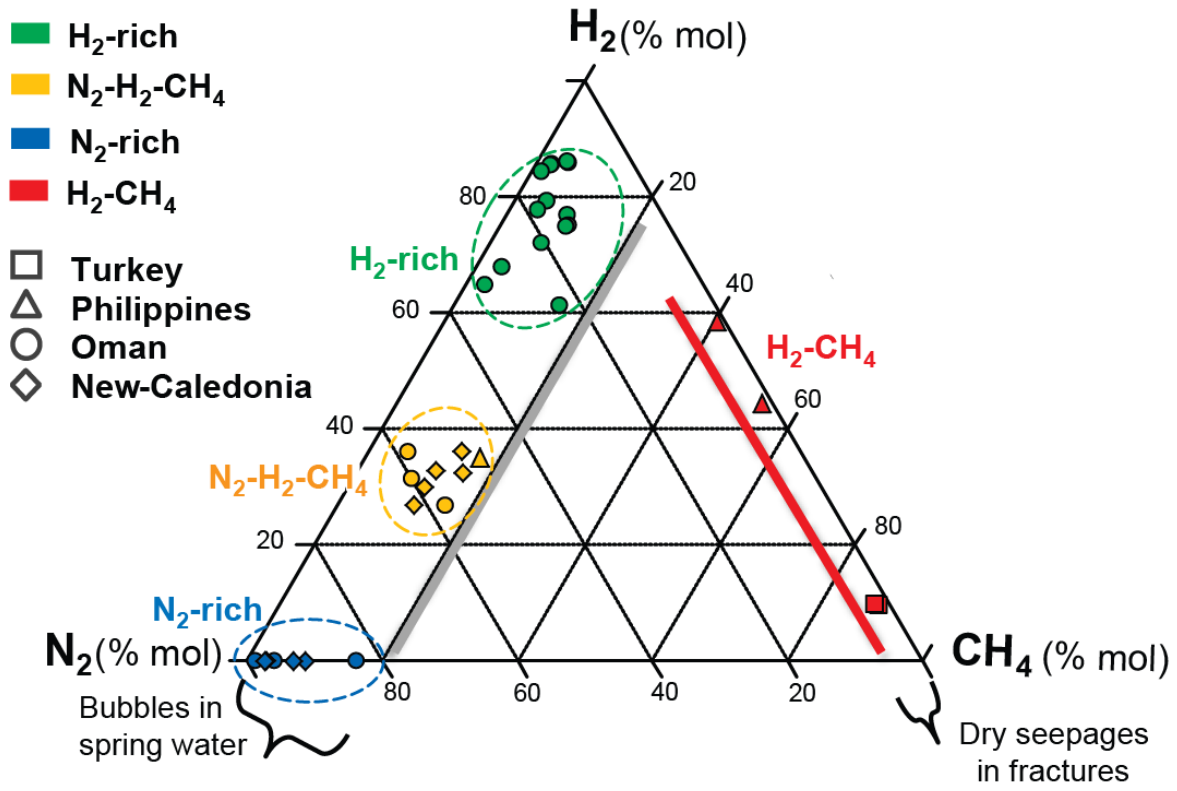

1216

1217 **Figure 4** - The major components of the gas mixtures sampled in Turkey, Oman, New
1218 Caledonia and the Philippines : H_2, N_2 and CH_4 in a triangular diagram (% mol). Four
1219 different types of gas mixtures can be defined according to the relative contents of H_2, N_2 and
1220 CH_4. Distinct chemical features correspond to distinct seepages styles : N_2-containing gas
1221 mixtures are associated with water and seep in water streams, whereas N_2-free mixtures
1222 correspond to dry seepages which seep out of fractures of massive rocks and locally ignite
1223 spontaneously. The different types of water-associated seepages correspond also to specific
1224 water physical properties, notably pH and temperature (see Fig. 5).

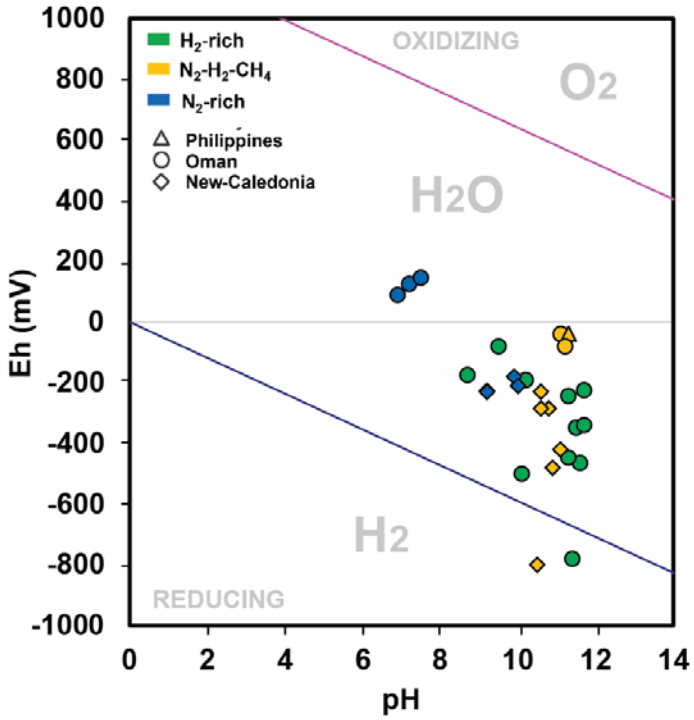

1225

1226 **Figure 5 -** Pourbaix diagram pH-Eh of the water where the gas samples were collected in
1227 springs. Oblique lines (blue and pink) separate the stability fields of H_2, H_2O and O_2.

1228

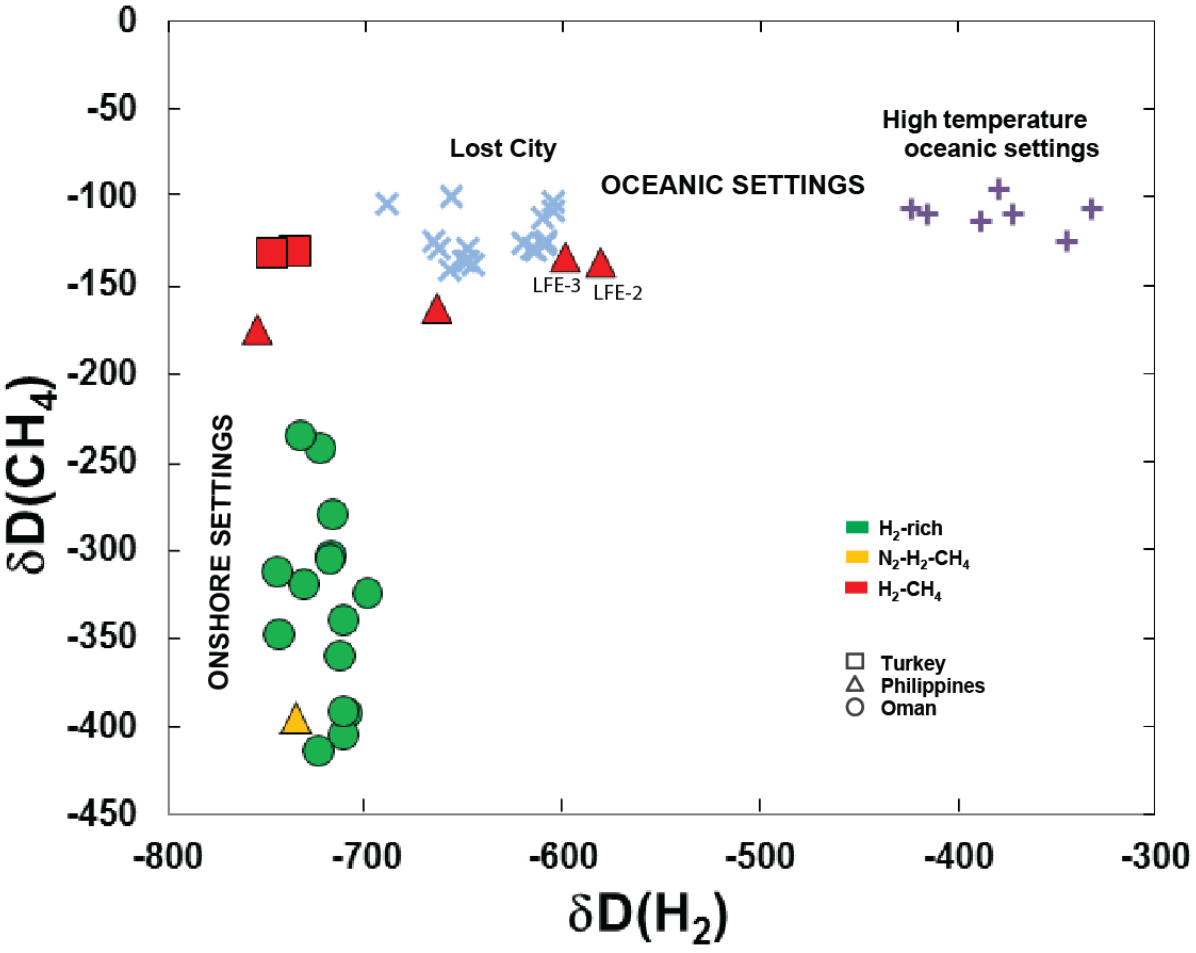

Figure 6 - Comparison of hydrogen isotopic compositions of CH_4 and H_2 for onshore settings (data from this work and two points, LFE-2 and LFE-3, from Abrajano et al., 1988) and oceanic settings (Proskurowski et al., 2006). While a narrow range of CH_4 isotopic composition is observed for oceanic settings these values are lower for onshore settings and cover a large range. The values for the gas seeping out of fractures without associated ultra-basic water (H_2-CH_4 gas type) are close to those of oceanic setting at Lost City and might indicate a similar generation process. In contrast to the CH_4 isotopic compositions, the H_2 isotopic compositions display a large range in oceanic settings (dependent on temperature) and a narrow range in terrestrial settings for gas seeping from ultra-basic springs.

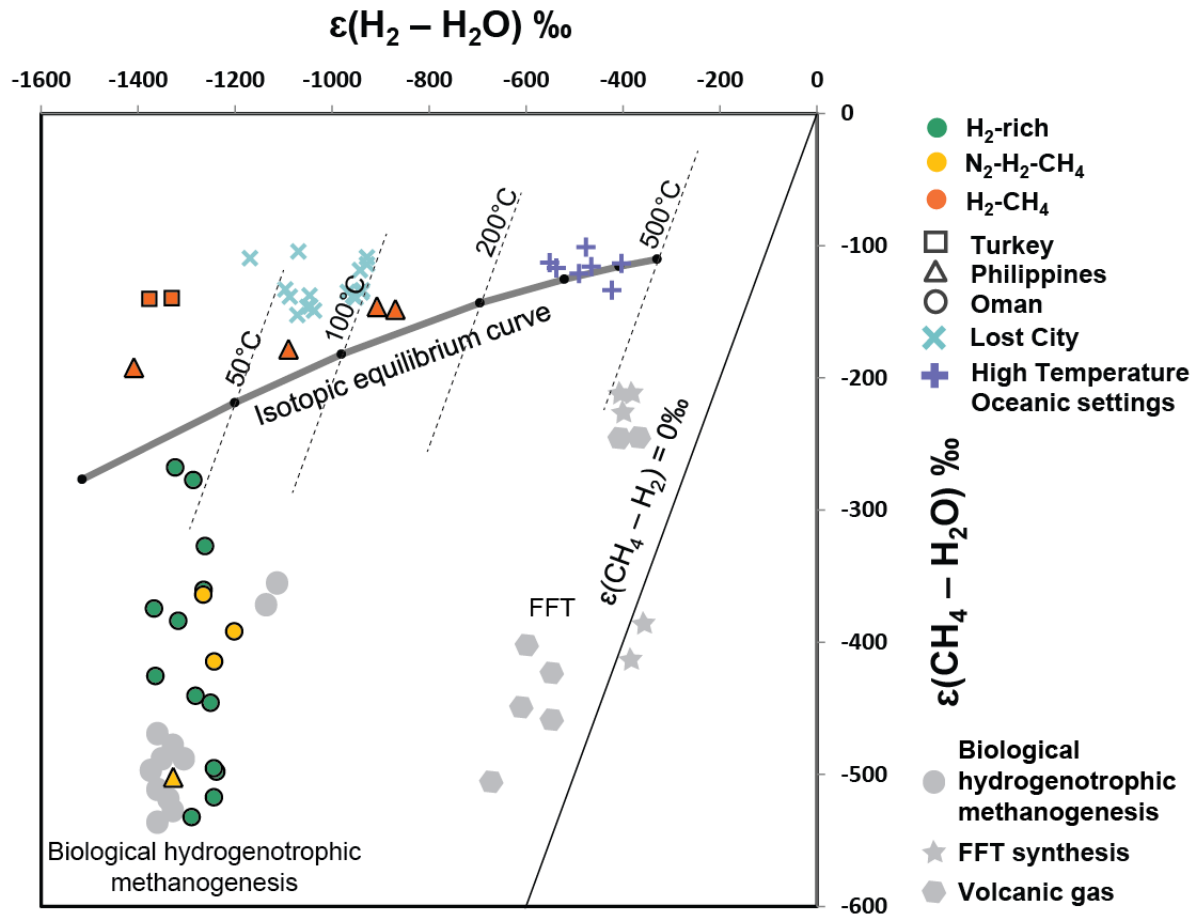

1243

1244 **Figure 7 -** CH_4-H_2-H_2O hydrogen isotope systematics. Data for biological hydrogenotrophic
1245 methanogenesis are from Balabane et al. (1987), Valentine et al. (2004) and Okumura et al.
1246 (2016). FTT synthesis refer to experiments investigating abiotic methane production in the
1247 gas phase (Taran et al., 2010) and aqueous phase (Fu et al., 2007; McCollom et al., 2010).
1248 There data were presented in a similar diagram in Suda et al. (2014). This figure shows Ɛ(H_2-
1249 H_2O_{aq}) versus Ɛ(CH_4-H_2O_{aq}) for the samples from Oman, the Philippines and Turkey,
1250 compared to values from oceanic settings. The value Ɛ is calculated according to the
1251 following equations : Ɛ=1000lnα with $\alpha(H_2O_{aq}\text{-}H_2) = 1.0473 + 201036/T^2 + 2.060 \times 10^9/T^4 +$
1252 $0.180 \times 10^{15}/T^6$ and $\alpha(H_2O_{aq}\text{-}CH_4) = 1.0997 + 8456/T^2 + 0.9611 \times 10^9/T^4 - 27.82 \times 10^{12}/T^6$.
1253 The thin line indicates the CH_4–H_2 equilibrium fractionation at a given temperature.
1254 According to this interpretation, CH_4 from fractures (dry seepages) would be produced
1255 directly from H_2O and DIC whereas, in the H_2-rich and N_2-H_2-CH_4 gas mixtures seeping in
1256 alkaline springs, an H_2 intermediate (possibly biologically mediated secondary process) would
1257 produce CH_4. δD of spring water is considered to be close to zero ‰ from the study made in
1258 Oman by Neal and Stanger (1985; values between -11.2 and +10.7‰).
1259

1260

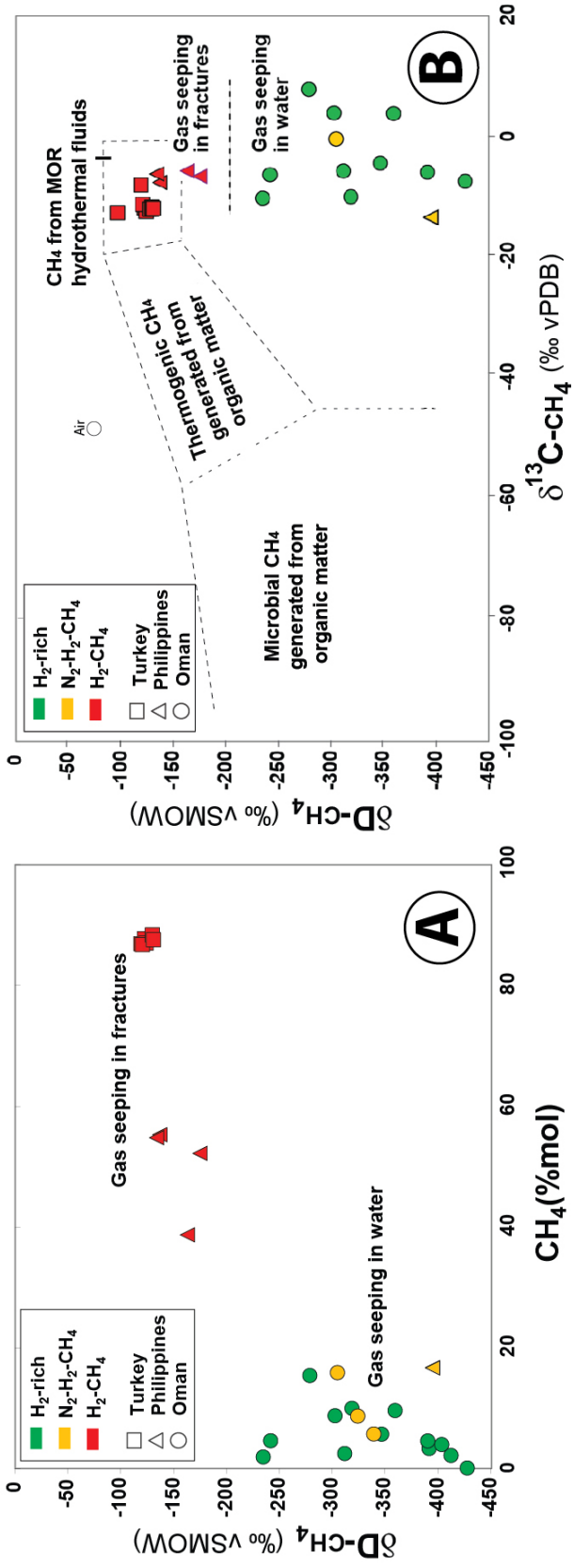

1261 **Fig 8**

1262

Figure 8 – A. Diagram showing δD(‰) values of CH_4 vs CH_4 contents. This shows that the H_2 -CH_4 gas type shows higher CH_4 contents and δD values of CH_4 than the other gas types. **B.** Diagram showing carbon versus hydrogen isotopic composition of CH_4 including data from Abrajano et al. (1988) and Hosgörmez et al. (2008), domains are simplified after Scholl (1983), Whiticar (1999), Etiope and Sherwood-Lollar (2013). The classic microbial domain presented here refers to gas generated from an organic substrate. This domain might be wider in the case of microbial gas generated from inorganic carbon. The carbon isotopic compositions of CH_4 are among the highest values recorded on Earth. The range of the carbon isotopic values of CH_4 is relatively narrow and allows no distinction between the different types of gas mixtures whereas the hydrogen isotopic values of CH_4 are scattered between -430‰ and -100‰ and show distinct ranges comparing dry seepages in fractures and seepages in ultra-basic water. This corresponds probably to different CH_4 generation processes. Note that none of the groups plot in the classical domains of conventional microbial gas or conventional thermogenic gases. Domain for CH_4 of Mid-Oceanic Ridges hydrothermal fluids is from Proskurowski et al. (2006) and Kawagucci et al. (2016).

1280

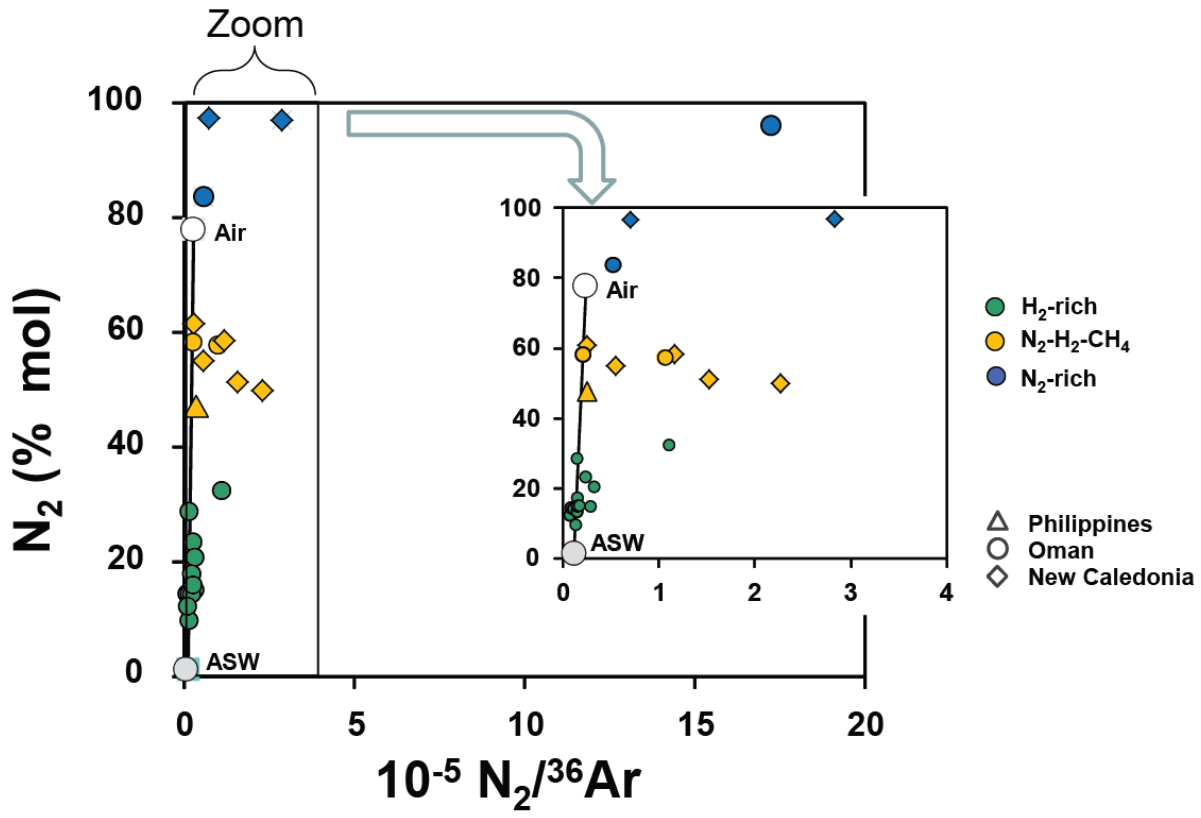

1281

1282 **Figure 9** - N_2 content *vs* $N_2/^{36}Ar$ diagram, depicting nitrogen excess in samples relative to
1283 atmospheric ^{36}Ar. The values from the H_2-rich type gather along a mixing line between air
1284 and air equilibrated water, implying that probably only inherited atmospheric N_2 can be found
1285 in the gas mixture, whereas the other types show a N_2 excess, suggesting that non-
1286 atmospheric N_2 is present in the gas mixture.

1287

1288

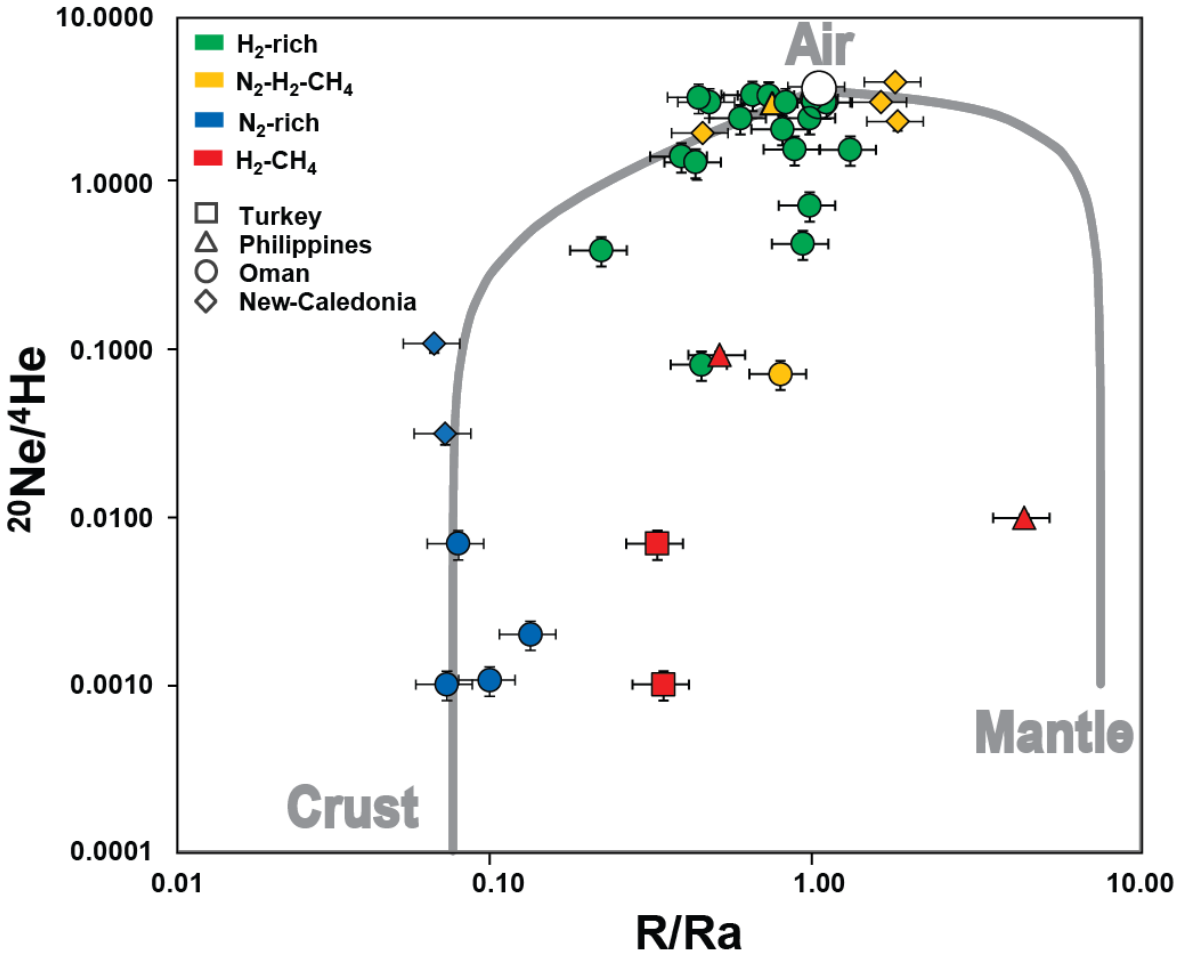

1289

1290 **Figure 10 -** Mixing diagram $^{20}Ne/^{4}He$ *vs* R/Ra ($^{3}He/^{4}He$ ratio of the sample normalized over
1291 the same ratio for the air = 1.384 x 10^{-6}). The noble gas data show that except the H_2-rich type
1292 which plots around the atmospheric end-member and indicates a single shallow aquifer
1293 signature, the other gas mixtures have signatures that result from the interaction of several
1294 fluids originating either from the mantle or from the crust. The N_2-rich type is interpreted as
1295 resulting from the mixing of atmospheric and crustal end-members whereas a mantle
1296 contribution is recorded for samples of the N_2-H_2-CH_4 and H_2-CH_4 types.

1297

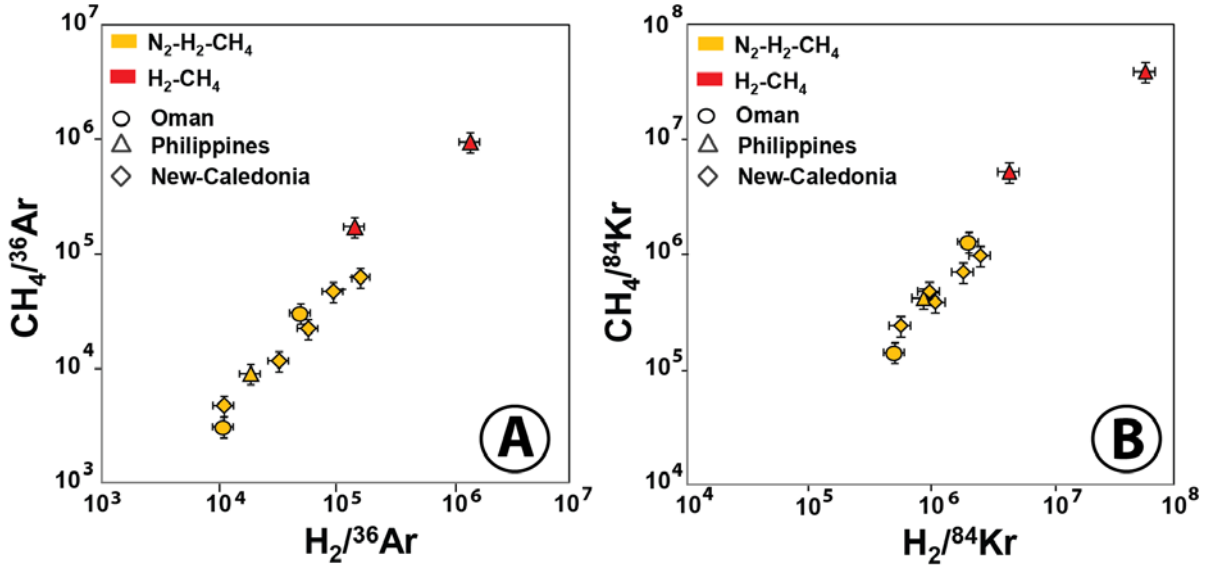

1298

1299 **Figure 11 –** Mixing diagrams comparing H_2 and CH_4 contents normalized over ^{36}Ar and ^{84}Kr
1300 contents. **A.** This diagram shows a correlated enrichment in CH_4 *vs* H_2 when normalized over
1301 ^{36}Ar (linear correlation with R^2= 0.9894). **B.** This diagram shows also a correlated enrichment
1302 in CH_4 *vs* H_2 when normalized over ^{84}Kr (linear correlation with R^2= 0.9953).

1303

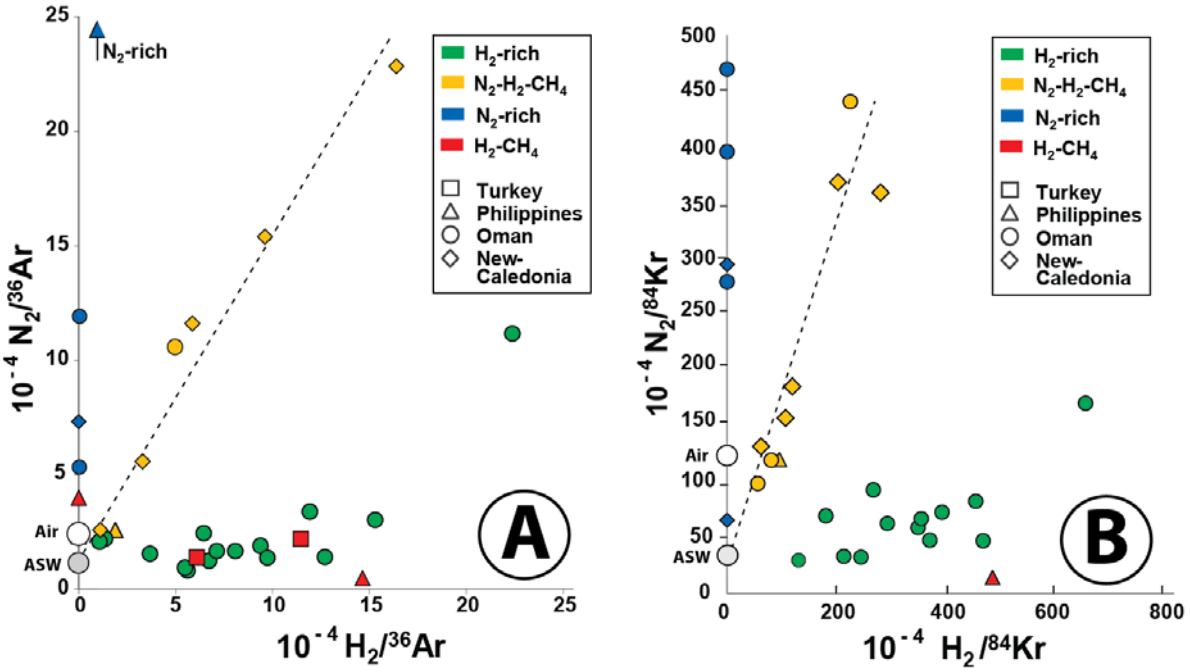

Figure 12 – Mixing diagrams comparing H_2 and N_2 contents normalized over ^{36}Ar and ^{84}Kr contents. **A.** The $H_2/^{36}Ar$ *vs* $N_2/^{36}Ar$ diagram shows different enrichment trends in H_2 *vs* N_2 between the H_2-rich gas type and the N_2-H_2-CH_4 gas type. Note the good linear correlation between $H_2/^{36}Ar$ *and* $N_2/^{36}Ar$ for the N_2-H_2-CH_4 gas type (linear correlation R^2= 0.9785). **B.** The $H_2/^{84}Kr$ *vs* $N_2/^{84}Kr$ diagram, as the previous diagram, shows different enrichment trends in H_2 vs N_2 between the H_2-rich gas type and the N_2-H_2-CH_4 gas type. Note the good linear correlation between $H_2/^{84}Kr$ and $N_2/^{84}Kr$ for the N_2-H_2-CH_4 gas type (linear correlation with R^2= 0.9739).

1316

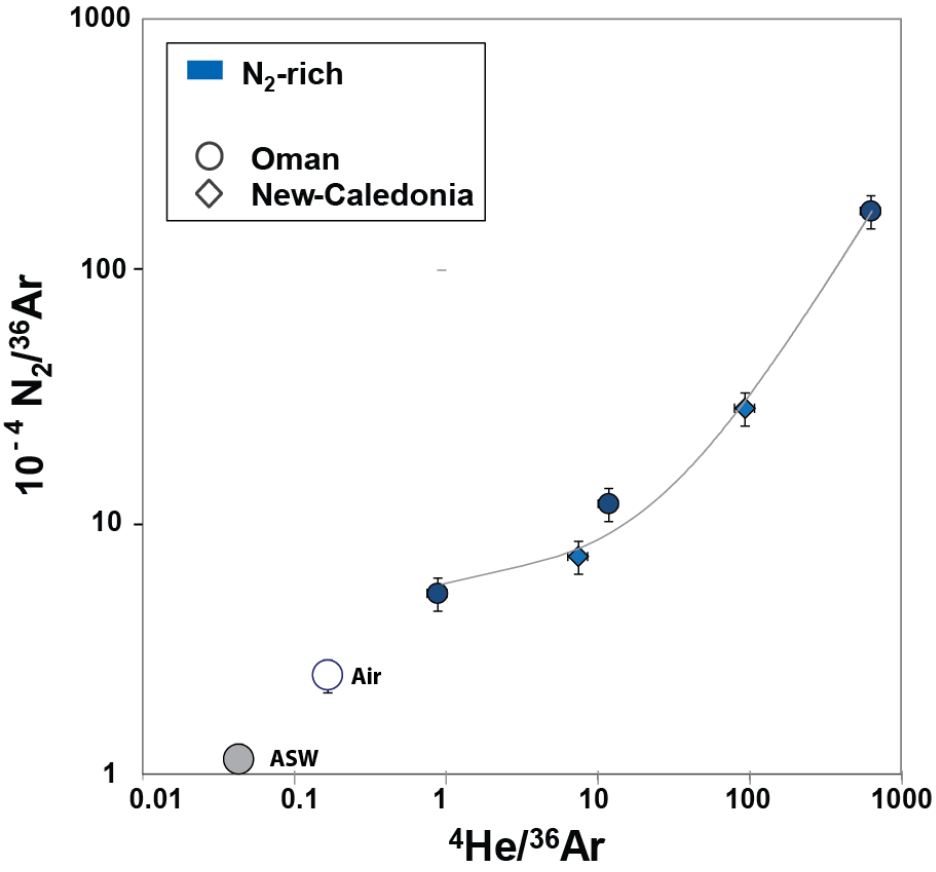

1317

1318

1319 **Figure 13 -** $^4He/^{36}Ar$ *vs* $N_2/^{36}Ar$ mixing diagram for the gas samples of the N_2-rich gas type.
1320 This diagram shows a correlated enrichment in ^4He *vs* N_2 when normalized over ^{36}Ar (linear
1321 correlation with R^2= 0.9993)

1322

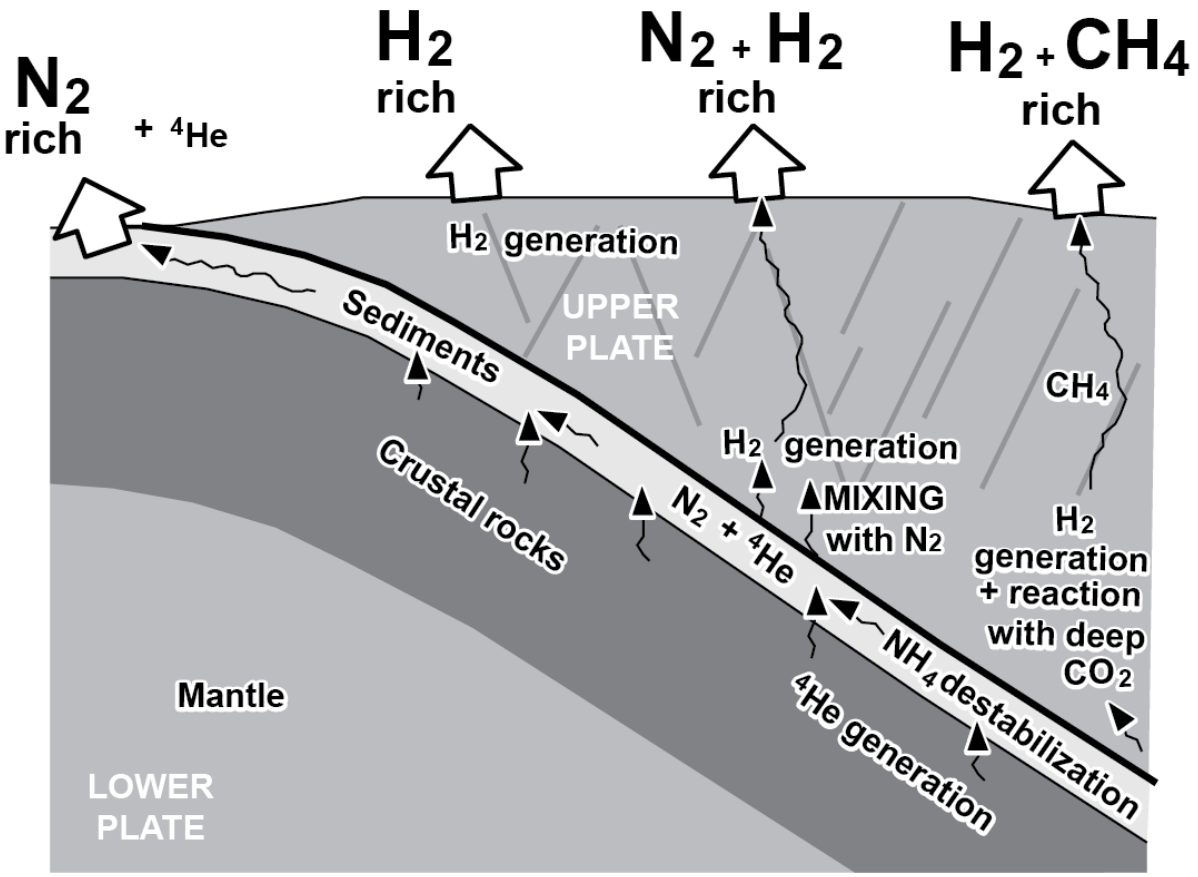

Figure 14 - Synthetic conceptual cross-section of an ophiolitic system with the different gas generation zones and different types of seepages.

In this interpretative sketch, H_2 is generated within the ophiolite at different depths by reduction of water, leading to different types of seepages depending on the other fluids interacting with H_2. When H_2 is generated in a shallow aquifer, it migrates upwards and seeps out of the rock as a H_2-rich gas seep. H_2 generated in a deeper generation zone interacts with deep fluids which can be (1) a N_2-rich fluid issued from the sediments and the mantle below, leading to a N_2 and H_2–rich gas, or (2) a fluid rich in CO_2, allowing the production of CH_4 and the formation of a gas mixture that seeps at the surface as a H_2-CH_4 gas seepages. N_2-rich seepages occur when the deep N_2-bearing fluid does not interact strongly with H_2-rich fluids on its migration pathway.

1337

	Sites	Coordinates		Water T, pH, Eh			gas composition					
		(decimal degrees)		(°C)		(mV)	Mol (%)					
		latitude	longitude	T	pH	Eh	He	H_2	N_2	CH_4	CO_2	C_{2+}
H_2-rich type												
Oman	Magniyat	23.4061	56.8633	32	11.7	-225	<0.01	87.3	9.8	2.9	<0.01	<0.01
	Hawasina	23.6833	56.9396	25.6	11.3	-244	<0.01	85.9	9.4	4.6	<0.01	<0.01
	Bahla 2008	22.9922	57.2932	35	11.6	-465	<0.01	85.7	12.4	1.9	<0.01	<0.01
	Bahla 2010	22.9922	57.2932	34.9	11.4	-780	-	-	-	-	-	-
	Bahla 2012	22.9922	57.2932	34.9	11.3	-447	<0.01	85.7	12.0	2.2	<0.01	0.02
	Kufeis	23.9588	56.4400	22.5	9.5	-80	<0.01	85.4	14.5	0.1	<0.01	<0.01
	Haylayn 2010	23.6199	57.1132	28.2	11.5	-348	<0.01	77.0	14.2	8.8	<0.01	<0.01
	Haylayn 2012-2a	23.6275	57.1152	-	-	-	<0.01	75.0	15.4	9.6	<0.01	<0.01
	Haylayn 2012-2b	23.6275	57.1152	-	-	-	-	-	-	-	-	-
	Haylayn 2012-6	23.618	57.1064	-	-	-	<0.01	77.8	18.1	4.0	0.05	0.05
	Haylayn 2012-8	23.6181	57.1078	-	-	-	<0.01	79.4	16.0	4.6	<0.01	0.01
	Barrage (Jizzi)	24.3282	56.1307	24.7	10.2	-191	<0.01	75.2	14.9	10.0	<0.01	<0.01
	Halhal	23.7172	57.034	27.7	8.7	-175	<0.01	73.4	20.8	5.8	<0.01	<0.01
	Alkar	23.9693	56.4219	31.5	11.7	-340	<0.01	68.1	28.5	3.3	<0.01	<0.01
	Huqain	23.5352	57.3333	31.2	10.1	-500	<0.01	65.1	32.4	2.5	<0.01	<0.01
	Lauriers Roses	22.8956	58.3946	29.5	11.2	-45	<0.01	61.0	23.2	15.4	<0.01	<0.01
N_2-H_2-CH_4 type												
Oman	Abyiad 2010	23.4285	57.6683	32.9	11.1	-420	<0.01	26.9	57.3	15.9	<0.01	<0.01
	Abyad 2012-29	23.4239	57.6722	23.8	11.1	-39	<0.01	36.1	58.2	5.7	<0.01	0.01
	Abyad 2012-30	23.4242	57.6721	37.4	11.2	-82	<0.01	31.4	59.9	8.7	<0.01	0.01
Philippines	Mangatarem	15.7033	120.2825	34.3	11.3	-38	<0.01	35.1	48.0	16.7	<0.01	<0.01
New Caledonia	Baie du Carénage1	-22.3047	166.8408	-	10.8	-285	<0.01	36.1	50.3	13.7	<0.01	<0.01
	Baie du Carénage2	-22.3047	166.8408	40.1	10.5	-800	<0.01	32.4	51.9	15.7	<0.01	<0.01
	Source des Kaoris 1	-22.2992	166.8617	31.6	10.9	-480	<0.01	26.8	61.9	11.3	<0.01	<0.01
	Source des Kaoris 2	-22.2992	166.8617	30.4	10.6	-230	<0.01	32.9	55.3	11.5	<0.01	<0.01
	Source des Kaoris 3	-22.2992	166.8617	30.5	10.6	-285	<0.01	29.8	58.9	11.3	<0.01	<0.01
N_2-rich type												
Oman	Al Ali	23.4701	58.3239	66.3	6.9	89	<0.01	<0.01	97.9	0.2	1.8	0.1
	Rustaq	23.3935	57.4113	45.3	7.2	125	0.2	<0.01	99.2	<0.01	0.7	<0.01
	Nakhal	23.3754	57.8284	37.9	7.5	146	0.1	<0.01	98.9	<0.01	1.0	<0.01
New Caledonia	La Crouen	-21.535	165.8889	41.5	9.2	-226	0.1	<0.01	97.2	2.7	<0.01	<0.01
	La Crouen	-21.535	165.8889	41.5	9.2	-230	0.1	<0.01	97.3	2.7	<0.01	<0.01
	Roc Aiguille	-22.3167	166.8333	23.5	9.9	-180	<0.01	0.1	93.1	5.1	1.7	<0.01
	Roc Aiguille	-22.3167	166.8333	23.5	10.0	-210	<0.01	<0.01	91.4	8.5	0.1	<0.01
H_2-CH_4 type												
Philippines	Nagsasa	14.837	120.1282	-	-	-	<0.01	58.5	1.2	38.7	<0.01	<0.01
	Los Fuegos Eternos	15.5718	120.1513	-	-	-	<0.01	44.5	1.5	52.2	<0.01	<0.01
Turkey	XI2	36.4318	30.4557	-	-	-	<0.01	9.4	1.8	88.4	<0.01	0.3
	XI3	36.4352	30.4532	-	-	-	<0.01	9.7	2.2	87.6	<0.01	0.3
Reference compositions												
air								5E-05	78.08	2E-04	0.04	
ASW								9E-07	1.23	6E-06	0.03	

1338

1339

1340 **Table 1**. Temperature, pH and Eh of the studied springs. Major gas analyses (mol%).

1341

	Sources/Wells	Per mil vs PDB		Per mil vs SMOW		Per mil vs atm	noble gases composition				
		$\delta^{13}C$		δD		$\delta^{15}N$	(ppm)				
		CO_2	CH_4	H_2	CH_4	N_2	^4He	^{20}Ne	^{36}Ar	^{84}Kr	R/Ra
H_2-rich type											
Oman	Magniyat	-	-12.8	-	-	-	-	-	-	-	-
	Hawasina	-	-6.2	-724	-242	-	1.87	-	6.76	0.20	0.77
	Bahla 12/2008	-	-10.1	-722	-235	-	2.50	3.687	15.19	0.38	0.37
	Bahla 01/2010	-	-	-734	-234	-	20.80	0.224	7.78	0.24	0.17
	Bahla 2012	-	-	-725	-413	-	1.16	0.864	8.80	0.25	0.93
	Kufeis	-	-7.3	-	-428	-	2.70	3.676	15.36	0.43	0.41
	Haylayn	-	4	-718	-303	-	9.43	3.800	11.41	0.24	0.21
	Haylayn 2a	-	3.9	-714	-360	-	0.96	1.552	9.28	0.23	0.84
	Haylayn 2b	-	-	-	-	-	1.31	2.819	8.33	0.22	0.77
	Haylayn 6	-	-	-712	-404	-	0.99	3.068	10.91	0.29	1.05
	Haylayn 8	-	-	-712	-391	-	0.64	2.079	8.45	0.22	0.95
	Barrage (Jizzi)	-	-9.9	-732	-319	-	15.27	1.260	4.91	0.18	0.43
	Halhal	-	-4.3	-744	-347	-	1.50	5.164	6.05	0.12	0.62
	Alkar	-	-5.8	-710	-392	-	2.85	9.750	18.44	0.41	0.70
	Huqain	-	-5.6	-745	-313	-	0.47	1.172	2.90	0.06	0.57
	Lauriers Roses	-	7.9	-717	-279	-	2.34	1.033	9.51	0.25	0.89
N_2-H_2-CH_4 type											
Oman	Abyiad	-	-0.3	-718	-305	-	7.43	0.543	5.41	0.13	0.76
	Abyaid 29	-	-	-711	-339	-	6.05	9.779	26.48	0.49	1.25
	Abyaid 30	-	-	-699	-324	-	3.47	8.680	28.90	0.61	0.93
Philippines	Mangatarem	-	-13.3	-735	-395	-0.1	2.66	8.204	18.62	0.40	0.71
New Caledonia	Baie du Carénage1	-	-32.4	-	-	-	3.88	14.967	2.20	0.14	1.00
	Baie du Carénage2	-	-	-	-	-	6.40	13.032	3.37	0.33	0.43
	Source des Kaoris1	-	-38.5	-	-	-	3.93	12.251	23.99	0.47	1.56
	Source des Kaoris2	-	-34.9	-	-	-	3.99	16.424	9.97	0.30	1.73
	Source des Kaoris3	-	-	-	-	-	3.99	9.550	5.08	0.16	1.76
N_2-rich type											
Oman	Al Ali	-	-	-	-215	-	14.10	12.559	16.03	0.30	0.42
	Rustaq	-16.5	-	-	-	-0.3	352.90	2.589	0.56	0.01	0.08
	Nakhal	-19.4	-	-	-	-	1382.07	1.760	12.12	0.25	0.07
New Caledonia	La Crouen	-	-39	-	-	-	320.92	10.392	3.42	0.33	0.07
	La Crouen	-	-39.2	-	-	-	99.37	11.047	13.30	1.48	0.06
	Aiguille de Prony	-	-12.1	-	-	-	-	-	-	-	-
	Aiguille de Prony	-	-16.4	-	-	-	-	-	-	-	
H_2-CH_4 type											
Philippines	Nagsasa	-	-5.6	-664	-163	0.5	4.68	0.047	0.41	0.01	4.35
	Los Fuegos Eternos	-	-6.5	-756	-175	-	4.38	0.419	3.04	0.10	0.49
Turkey	Turkey XI2	-	-11.8	-736	-130	-	151.2	1.098	0.82	0.01	0.31
	Turkey XI3	-	-11.8	-748	-131	-	140.5	0.080	1.59	0.02	0.33
reference compositions											
air		−8.6 to −7.6	−47.7 to −41.2	+100 to +200	-70 to -90	0	5.24	16.453	31.57	0.65	1
ASW							0.05	0.172	1.07	0.04	1

Table 2. $\delta^{13}C$ (PDB) values of CO_2 and CH_4 (‰). δD (SMOW) values of H_2 and CH_4 (‰). Noble gas analyses ^{4}He, ^{20}Ne, ^{36}Ar, ^{84}Kr (ppmv), and R/Ra (helium isotopic ratios normalized to the air isotopic $Ra=^{3}He/^{4}He=1.4\ 10^{-6}$). C2+ contents in all the gas samples are very low, below the threshold of analytical precision (< 0.01%). Global relative uncertainties (at 1σ) for quantification of noble gases with the method used is estimated in the range He: ±10%; Ne: ±20%; Ar: ±5%; Kr: ±10%. The global relative uncertainty (1σ) for the R/Ra ratio is in the range ±2%.

SUPPLEMENTARY MATERIAL.

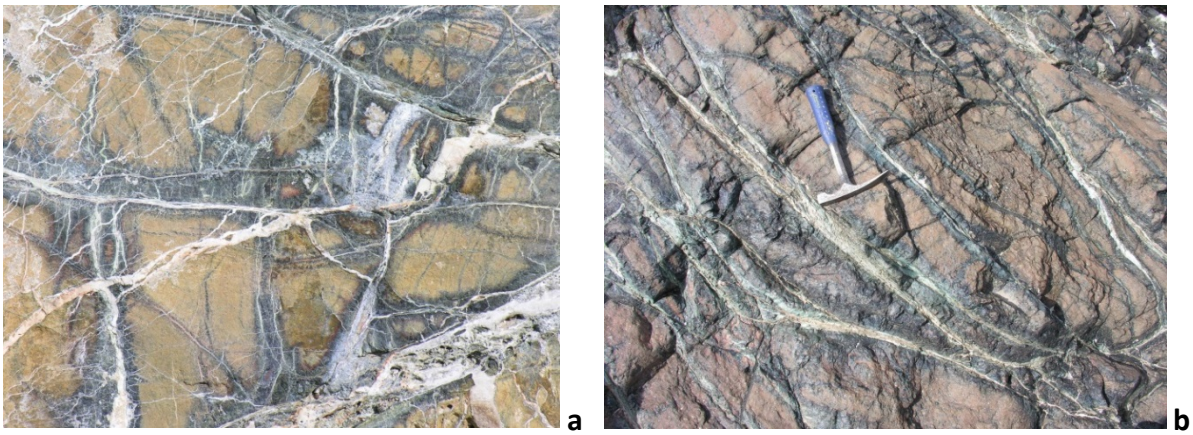

Figure S1 a and b- Photos illustrating alteration processes in the peridotites of Oman. Brow zones correspond to poorly serpentinized peridotites, black zones correspond to serpentinized parts along the fractures which are filled by Mg-Ca carbonate cements.

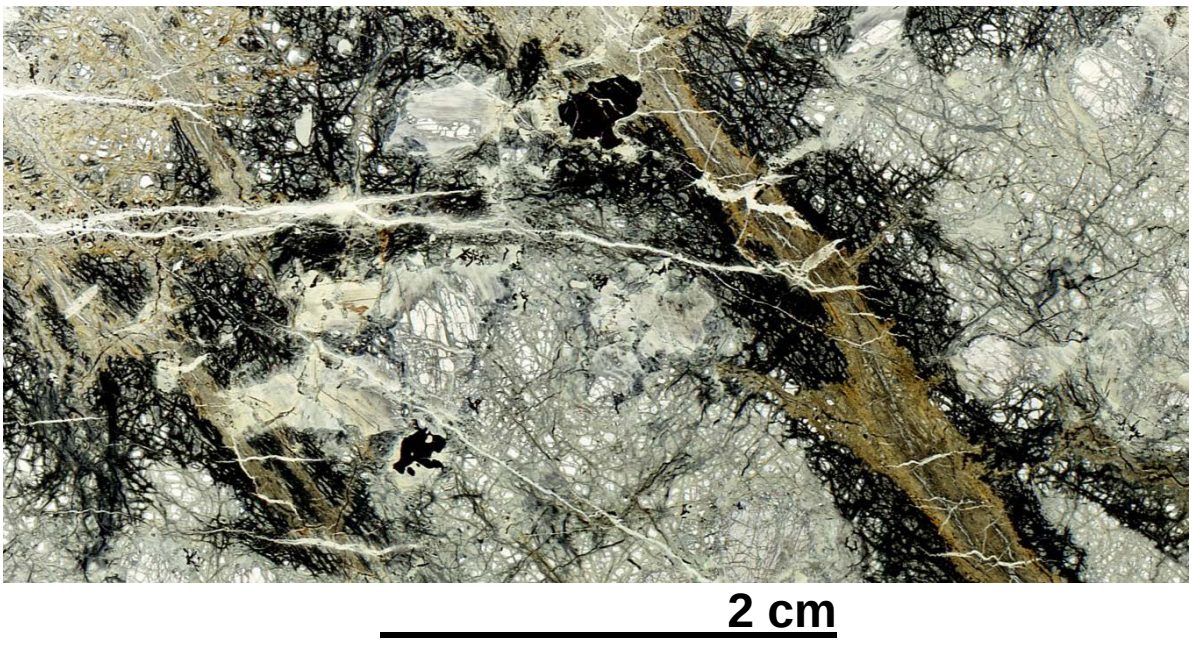

Figure S2 - Photo of a thin section illustrating alteration processes in the peridotites of Oman. grey zones correspond to poorly serpentinized peridotites, black zones correspond to serpentinized parts along the fractures which are filled by Mg-Ca carbonate cements which appear in brown.

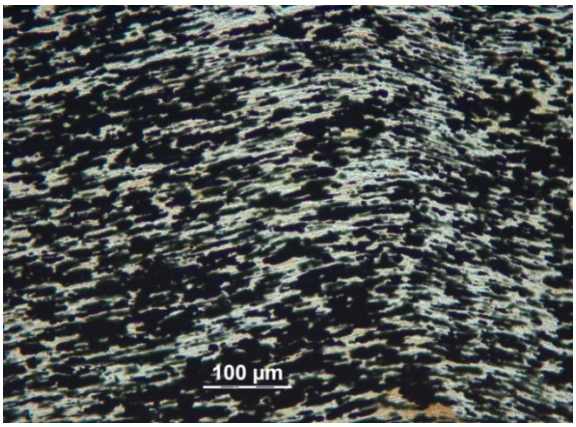

a

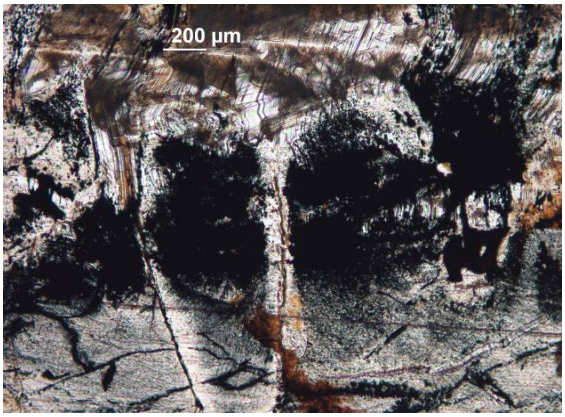

b

Figure S3 a and b - Photos of thin sections showing magnetite aggregates.

Figure S4 - An example of a blue pool in Oman (Sayah). Note the blue color related to the formation of carbonates in water. A precipitate of aragonite and brucite is observed at the bottom of the basin.

Figure S5 - Another example of a blue pool in Oman. The water in these basins shows pH values generally between 11 and 12. A film of calcite develops on the water surface and a precipitate of aragonite and brucite is deposited at the bottom of the basin.

Figure S6 - Calcite film appearing on the surface of ultra-basic water (Oman).

1383

1384

1385 **Figure S7 -** Aragonite precipitation in ultra-basic water (Oman).

1386

1387 **Figure S8 -** Aragonite chimneys forming in ultra-basic water (Oman).

1388

1389

1390

1391 **Figure S9 -** Needles of primary Brucite in the foreshore of the Baie des Kaoris (New
1392 Caledonia).

1393

1394

Sample	δ18O	δ13C	Type of rock	RXD
WAA3	11.53	2.19	Carbonated peridotite	magnesite
O26A	33.19	8.15	Carbonate cement in fracture	magnesite
O2	31.18	-8.28	Carbonate cement in fracture	dolomite
WAA1	29.58	-6.65	Carbonate cement in fracture	dolomite
O1	30.2	-6.53	Carbonate cement in fracture	dolomite
O35B	28.99	-12.47	Surface carbonate crust	aragonite, calcite
O16A	23.57	-9.14	Surface carbonate crust	calcite
O31	29.21	-8.91	Surface carbonate crust	aragonite
O18	28.96	-8.16	Surface carbonate crust	dolomite, calcite
O11	18.11	-4.15	Surface carbonate crust	calcite
O10	23.87	-1.48	Surface carbonate crust	calcite
O23B	29.29	-10.51	Surface carbonate crust	aragonite, dolomite

1395

1396 **Table S1 -** $\delta^{13}C$ PBD (‰) and $\delta^{18}O$ SMOW (‰) of carbonate rocks (carbonated peridotite,
1397 carbonate cement in fracture, surface carbonate crust) associated with the ophiolites of Oman.

1398